

A
Report
On
“FREE VIBRATION ANALYSIS OF FGM CIRCULAR PLATE”

Submitted to
Department of Mechanical Engineering
in partial Fulfilment of requirement for the degree of
Bachelor of Technology

Submitted By

Anand Jain (Admission No. U17me207)

Manali Bajaj (Admission No. U17me221)

Mahendra Singh (Admission No. U17me210)

Soham Sharma (Admission No. U17me219)

Under the Supervision of

Dr. SUMIT KHARE



DEPARTMENT OF MECHANICAL ENGINEERING
SARDAR VALLABHBHAI NATIONAL INSTITUTE OF
TECHNOLOGY SURAT-395007, GUJARAT, INDIA



CERTIFICATE

This is to certify that the project report entitled “Free Vibration Analysis of FGM Circular Plate” submitted by Anand Jain (U17ME207), Manali Bajaj (U17ME221), Mahendra Singh (U17ME210) and Soham Sharma (U17ME219) in fulfilment for the award of the degree in “Bachelor of Technology in Mechanical Engineering” during the Academic year 2020-2021, of the Sardar Vallabhbhai National Institute of Technology, Surat is a record of their own work carried out under our supervision and guidance.

Dr. Sumit Khare

Assistant Professor, MED
SVNIT, Surat

Dr. Jyotirmay Banerjee

Head of Department, MED
SVNIT, Surat



EXAMINER'S APPROVAL CERTIFICATE

This is to certify that the project entitled “Free Vibration Analysis of FGM Circular Plate via Differential Quadrature Method” submitted by **U17ME207, U17ME210, U17ME219, U17ME221** in fulfilment for the award of the degree of Bachelor of Technology in Mechanical Engineering Department during the Academic year 2020-21, at the Sardar Vallabhbhai National Institute of Technology, Surat is hereby approved for the award of the degree.

Examiners:

1.)Dr. Sandeep Soni

2.)Mr. Anil Mahto

3.)Mr. Nikunj Patel

Date:

Place:

ACKNOWLEDGEMENT

The completion of this project would not have been possible without the kind support and help of many individuals of our institute. We would like to extend sincere thanks to all of them.

Firstly, we would like to express a sense of immense gratitude towards our respected guide **Dr. Sumit Khare, Assistant Professor, MED, SVNIT** for his guidance and constant perspective supervision as well as for providing necessary information regarding the project and his everlasting support in completing this project. We also express our regards to **Dr. S.K. Budhwar, Professor, Head of the Mechanical Engineering Department SVNIT, Surat.**

We would like to express our gratitude towards our parents and friends for their full support.

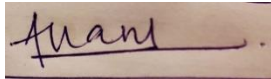
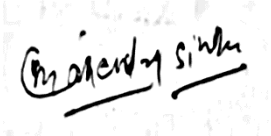

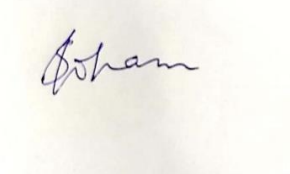
Sr. No.	Admin. No.	Name	Signature
1.	U17ME207	Anand Jain	
2.	U17ME210	Mahendra Singh	
3.	U17ME221	Manali Bajaj	
4.	U17ME219	Soham Sharma	

Table of contents

CERTIFICATE	2
EXAMINER’S APPROVAL CERTIFICATE	3
ACKNOWLEDGEMENT	4
TABLE OF CONTENTS	5
LIST OF FIGURES	6
LIST OF TABLES	7
ABSTRACT	8
1. INTRODUCTION	9
1.1 Types of plates	10
1.1.1 Based on Shape or Geometry	10
1.1.2 Based On Thickness	11
1.1.3 Based On Material Properties	11
1.2 Functionally Graded Materials (FGM)	14
1.3 Power Law	16
1.4 Plate Theories	17
1.4.1 Classical Plate Theory (CPT):-	20
1.4.2 First Order Shear Deformation Theory (FSDT)	24
1.5 Differential Quadrature Method (DQM)	25
1.6 Organization of the Report	26
2. LITERATURE REVIEW	27
3. MATHEMATICAL FORMULATION	32
3.1 Introduction	32
3.2 Plate description	32
3.3 Strain displacement relations	34
3.4 Constitutive equations	35
4. SOLUTION METHODOLOGY	38
5. RESULT AND DISCUSSION	43
5.1 Free Vibration Analysis of FGM Circular Plate	43
6. CONCLUSION	51
7. REFERENCES	52

List of Figures

Figure 1. Plate and associated stress components on an element [1]	9
Figure 2. (a) Triangular Plate, (b) Rectangular Plate, (c) Square/Rectangle Plate (d) Circular Plate	10
Figure 3. 3D geometry of the laminated composite plates [2]	12
Figure 4. Geometry and notations of a sandwich plate [3]	13
Figure 5. The functionally graded plate model [4]	13
Figure 6. Classification of FGM based on structure [6]	15
Figure 7. Plane stress loading of a plate	17
Figure 8. A Plate subjected to Lateral Loading	17
Figure 9. Deformed line elements remain perpendicular to the mid-plane	18
Figure 10 . The positive coordinate directions, stress resultants, and kinematic deformation of an edge in CPT and FSDT	19
Figure 11. The geometry of the circular FGM plate with five type of porosity distribution models.	34
Figure 12. Convergence and comparison study of C-C PFGM-1 annular plate	46
Figure 13. Influences of porosity index on fundamental frequency of PFGM-2 S-S circular plate with different porosity distribution type ($n=1$, $R_o=10, R_i=1, h=0.1$)	46
Figure 14. Influences of porosity index on fundamental frequency of PFGM-2 C-C circular plate with different porosity distribution type ($n=1$, $R_i/R_o=0.1$, $R_o/h=100$)	47
Figure 15. Influences of R_o/h ratio on fundamental frequency of PFGM-2 S-S circular plate with different porosity index ($n=1$, $R_o=10$, $R_i=1$, PD-1)	48
Figure 16. Influences of grading index on fundamental frequency of PFGM-2 S-S circular plate with different porosity index ($R_o=10$, $R_i=3$, $R_o/h=10$, PD-2)	48

List of Tables

Table 1. Mechanical properties of metallic and ceramic materials considered	43
Table 2. Convergence and validation studies of fundamental frequency of isotropic circular plate. (Simply Supported plate)	44
Table 3. Convergence and validation studies of fundamental frequency of isotropic circular plate. (Clamped plate)	45
Table 4. Influence of R_i/R_o ratio on fundamental frequency of PFGM-2 S-S circular plate with different porosity index ($R_o/h=20$, PD-3, $por=0.02$, $n=0.5$)	49
Table 5. Influence of R_i/R_o ratio on fundamental frequency of PFGM-2 C-C circular plate with different porosity index ($R_o/h=20$, PD-3, $por=0.02$, $n=0.5$)	50

Abstract

In this work, we have presented the numerical results for free vibration response of porous functionally graded circular plate using differential quadrature method. The displacement field is based on first-order shear deformation theory with five unknown variables. The Hamilton principle is used for finding the general governing differential equation. The effective material properties of porous FGM plate are obtained by modifying power law. After finding the governing differential equations for the circular plate, it is discretized using the differential quadrature method to obtain the eigenvalue problem for such a model plate for simply supported and clamped boundary conditions. By solving these eigenvalue problems using MATLAB the effect of grading index, boundary condition, porosity index and porosity distributions on the vibration response has been analyzed.

Keywords: Free vibration, circular plate, PFGM, differential quadrature method, porosity, porosity distribution.

1. Introduction

A plate is a structural element which is characterized by a three-dimensional solid whose thickness is very small when compared with other dimensions. Plates find extensive use in architectural structures, bridges, hydraulic structures, pavements, containers, airplanes, missiles, ships, instruments, machine parts, etc. Thin plates are flat structural members bounded by two parallel planes, called faces, and a cylindrical surface, called an edge or boundary. The generators of the cylindrical surface are perpendicular to the plane faces. The distance between the plane faces is called the thickness (h or t) of the plate **Figure 1**. It will be assumed that the plate thickness is small compared with other characteristic dimensions of the faces (length, width, diameter, etc.). Geometrically, plates are bounded either by straight or curved boundaries.

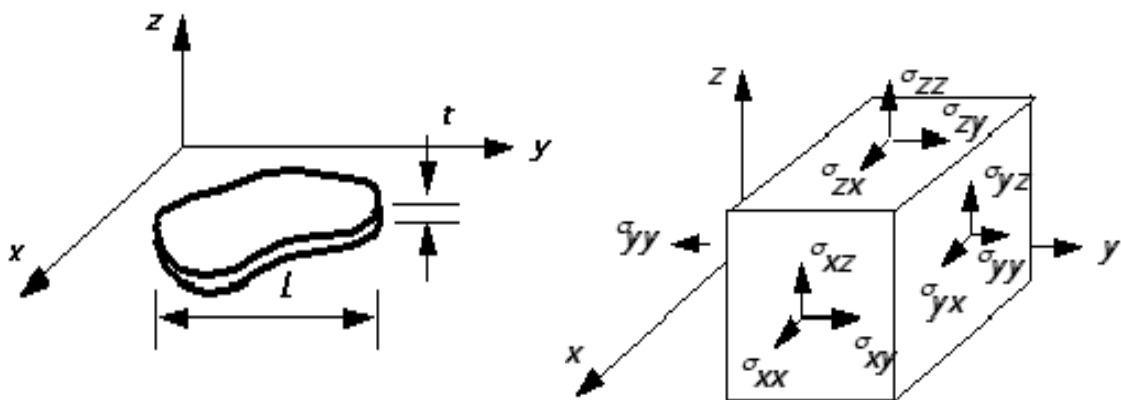


Figure 1. Plate and associated stress components on an element [1]

1.1 Types of plates

Depending on the application, different plates are required, it may be of a different shape, or a different size or a different material property. The plates can be classified under following headings: -

1.1.1 Based on Shape or Geometry

Structural members, common in engineering practice, consist of plates with shapes other than rectangular or circular as per the application (**Figure 2**).



Figure 2. (a) Triangular Plate, (b) Rectangular Plate, (c) Square/Rectangle Plate (d) Circular Plate

1.1.2 Based On Thickness

A plate may be classified based on its thickness to span ratio. If the thickness of a plate is very large compared to its length, it is a thick plate. Generally, the thickness to span ratio given by $\frac{h}{l}$ decides the relative thickness of the plates.

$$\frac{h}{l} \leq 0.05 : - \text{Thin Plates}$$

$$0.05 \leq \frac{h}{l} \leq 0.2 : - \text{Moderately thick Plates}$$

$$0.2 \leq \frac{h}{l} : - \text{Thick Plate}$$

1.1.3 Based On Material Properties

Each kind of plate is applicable for a specific use pertaining to requirements of strength and application. Physically the plate is classified according to its shape and size but the material properties play a vital role in the plate's strength and applicability.

1. **Homogeneous plate:** A material plate made up of a uniform composition throughout that cannot be mechanically separated into different materials. Examples of homogeneous materials are certain types of plastics, ceramics, glass, metals, alloys, paper, board and resins.
2. **Isotropic plate:** Properties of a material plate are identical in all directions. Glass and metals are examples of isotropic materials.
3. **Orthotropic plate:** Orthotropic plate materials have material properties that differ along three mutually orthogonal two-fold axes of rotational symmetry. E.g.: wood.

4. **Anisotropic plate:** Materials that are direction-dependent and are made up of unsymmetrical crystalline structures. In other words, the mechanical properties of anisotropic materials depend on the orientation of the material's body. Plate have different physical properties in different directions; for example, wood.
5. **Composite Plates:** A composite material plate is produced from two or more constituent materials with notably dissimilar chemical or physical properties that, when merged, create a component with properties unlike the individual elements. They can be further classified into:
 - (a) **Laminated Plates** - A laminated plate is an assembly of layers of fibrous composite materials which can be joined either by mechanical means like clamping or welding to provide required engineering properties, including in-plane stiffness, bending stiffness, strength, and coefficient of thermal expansion **Figure 3.**

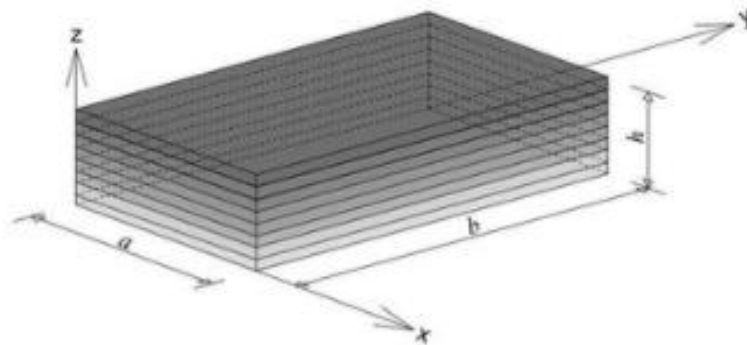


Figure 3. 3D geometry of the laminated composite plates [2]

(b) **Sandwich Plates** - A sandwich-structured composite is a special class of composite materials that is fabricated by attaching two thin but stiff skins to a lightweight but thick core. The core material is normally low strength material, but its higher thickness provides the sandwich composite with high bending stiffness with overall low density **Figure 4.**

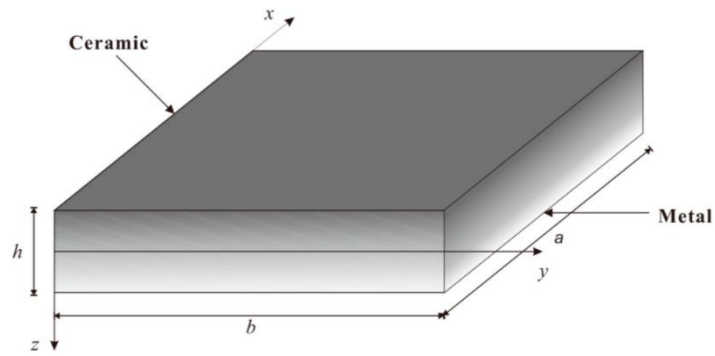


Figure 4. Geometry and notations of a sandwich plate [3]

(c) **FGM plates** – Functionally graded material (FGM) plate is a unique composite that displays a continuous or a stepwise variation of material properties which results in a non-homogenous, application-oriented, microstructure composition **Figure 5**.

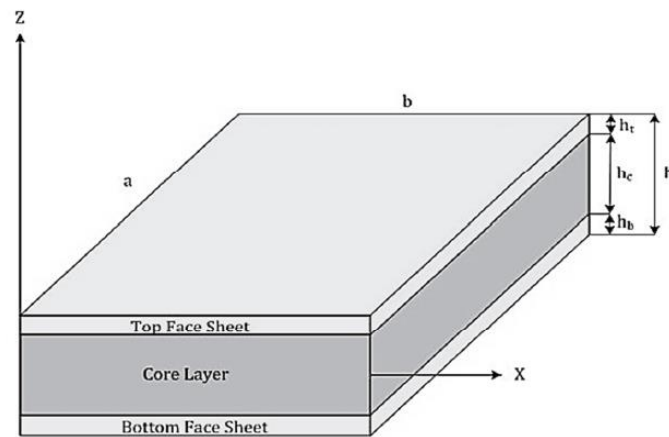


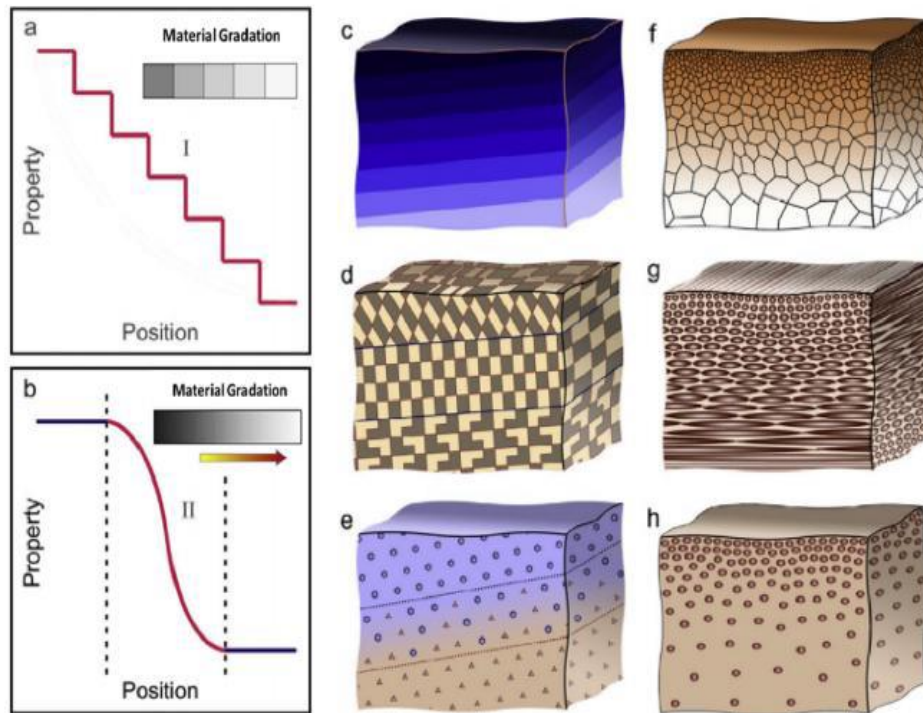
Figure 5. The functionally graded plate model [4]

1.2 Functionally Graded Materials (FGM)

The search of lightweight as well as stronger materials has constantly been a matter of prime concern to engineers worldwide. The necessity to upgrade conventional materials with modern or advanced ones stem from the upgraded requirement in the structural industry. Functionally Graded Materials (FGMs) are composed of two or more materials whose volume fraction changes gradually according to a predefined function along desired spatial directions resulting in a smooth and continuous change in the effective properties. The combination of different materials with specific physical properties allow for a tailored material design that broadens the structural design space by implementing a multi-functional response with a minimal weight increase. The scientific term “functionally graded material” was first coined in Japan in 1984 for development and connotation of thermal barrier materials [5]. A research project in Japan for a space shuttle put forth a fundamental study on the relaxation of thermal stress by tailoring graded Structures. The capacity of withstanding a surface temperature of 17000°C and a temperature gradient of 10000°C across merely a 10mm section led to the development of a unique composite called a functionally graded material. Under such drastic working conditions, delamination (separation of fibers from the matrix) in composites is the major drawback leading to the fracture of material. Since FGM has a continuous gradation in properties, it removes the problem of delamination.

FGM finds applications in aerospace, automobiles, marine, robots, rocket engine, turbine, aeronautics, nuclear, marine, defense, and the various other industries. For the last two decades there has been a significant research reports on mechanical response, buckling, free vibration, etc. of FGM structural elements such as plates and shells.

On the basis of FGM structure a continuous or a layered graded material as shown in



(a) Discrete/Discontinuous FGMs with interface (b) Continuous FGMs with no interface
(c , f) Composition Gradient (d , g) Orientation Gradient (e , h) Fraction Gradient

Figure 6 can be synthesized. In the continuous FGM, separation cut lines can't be observed inside the material to distinguish the properties of each zone.

Figure 6. Classification of FGM based on structure [6]

Whereas in layered FGM, material ingredients change in a discontinuous stepwise gradation. Continuous and discrete types can further be classified into three types: composition gradient, orientation and volume fraction gradient.

1.3 Power Law

In this paper effective material properties of metal ceramic functionally graded plates are varied through power law.

A power law is a functional relationship between two quantities, where a relative change in one quantity results in a proportional relative change in the other quantity, independent of the initial size of those quantities: one quantity varies as a power of another.

A FG plate is made from a mixture of two material phases, for example, a metal and a ceramic. The material properties of FG plates are assumed to vary continuously through the thickness of the plate and the property gradation through the thickness of the plate is assumed to have the following form:

$$Y(z) = [Y_c - Y_m] \left(\frac{2z + h}{2h} \right)^n + Y_m$$

Where Y represents the effective material property such as Young's modulus E , Poisson's ratio ν , and mass density ρ ; subscripts c and m denote the ceramic and metal phases, respectively. 'n' is the volume fraction exponent and 'h' is the thickness of the plate.

1.4 Plate Theories

Plates are defined as plane structural elements with a small thickness compared to the planar dimensions. The typical thickness to width ratio of a plate structure is less than 0.1 [7]. Plate theory takes advantage of this disparity in length scale to reduce the full three-dimensional solid mechanics problem to a two-dimensional problem. The aim of plate theory is to calculate the deformation and stresses in a plate subjected to loads.

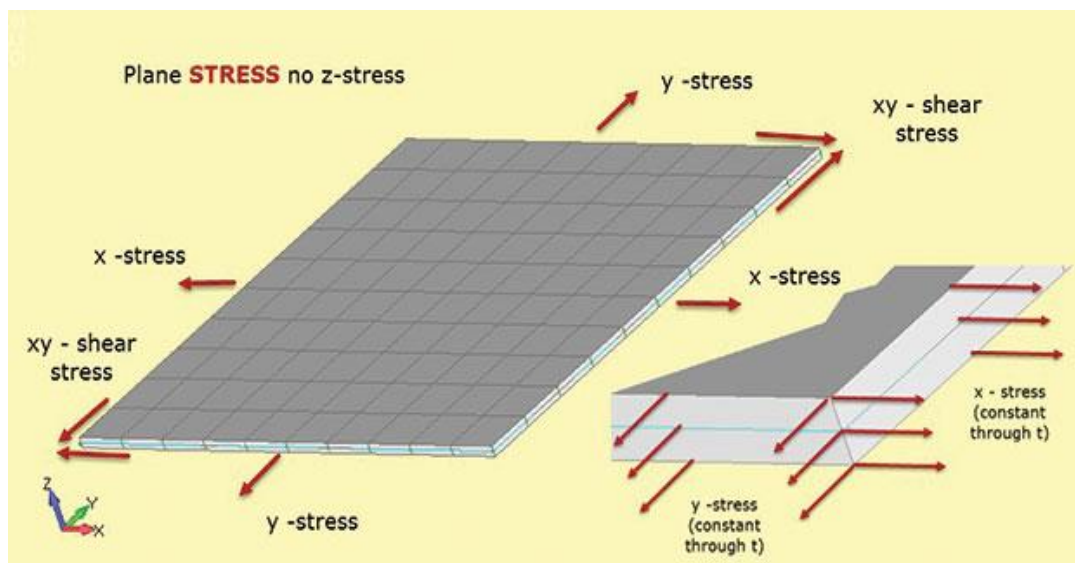


Figure 7. Plane stress loading of a plate

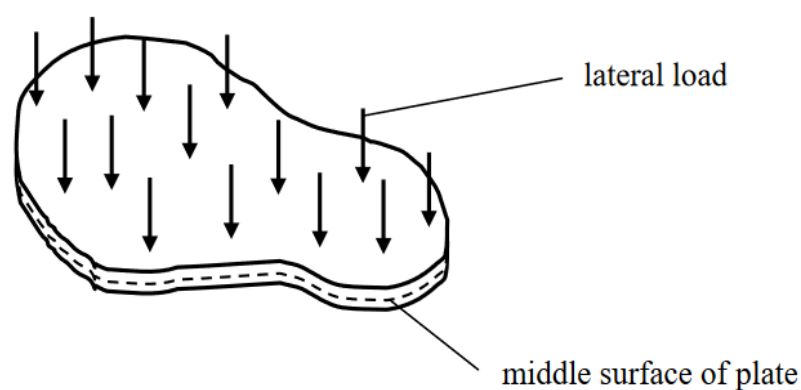


Figure 8. A Plate subjected to Lateral Loading

Plates subjected only to in-plane loading can be solved using two-dimensional plane stress theory. On the other hand, plate theory is concerned mainly with lateral loading. One of the differences between plane stress and plate theory is that in the plate theory the stress components are allowed to vary through the thickness of the plate, so that there can be bending moments.

Numerous Equivalent single layer theories (ESL) have been developed since the late 19th century, from these Equivalent single layer theories (ESL) two theories are widely accepted and used in engineering. These are:

1. The Kirchhoff–Love theory of plates (classical plate theory)
2. The Uflyand-Mindlin theory of plates (first-order shear plate theory)

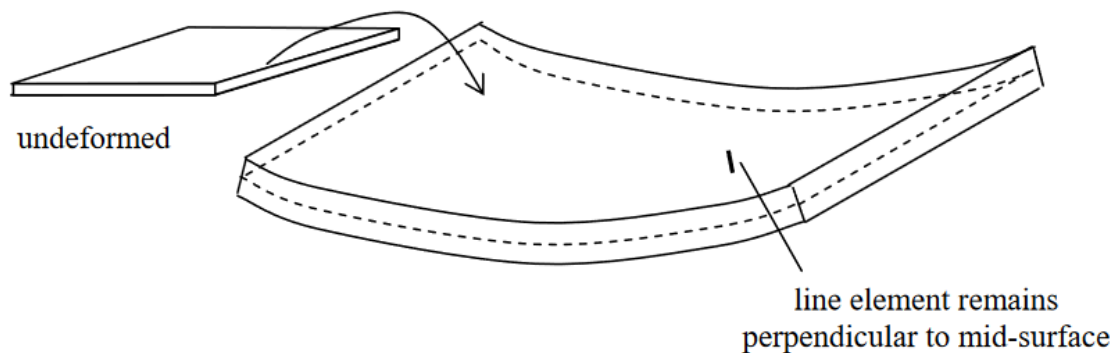


Figure 9. Deformed line elements remain perpendicular to the mid-plane

With the aim to discover the behavior of plates, different models have been developed and introduced in the past decades. Equivalent single layer theories (ESL) have been evolved to explore the behavior of plates or shells under the mechanical environment. Kirchhoff's theory is the basic and simple theory which is also identified as Classical Plate Theory (CPT), it neglects deformation due to shear effects. It explains that the plane at the center of the plate remains linear both before and after deformation. Thus, for CPT, thickness, shear and normal deformations are neglected. Further research led to

the development of improved first-order shear deformation theory (FSDT) which is otherwise called as Mindlin Shear Deformation Theory, which takes account of shear deformations, unlike CPT. For a plate, FSDT involves the linear distribution of plane displacements along thickness. FSDT is applicable for plates which are thin or thick up to some extent.

For thin plates: $\frac{h}{l} \leq 0.05$, thin plate theory- Kirchoff's classical plate theory (CLPT) & for moderately thick plates: $\frac{h}{l} \leq 0.2$, Reissner-Mindlin plate theory (FSDT) can be used.

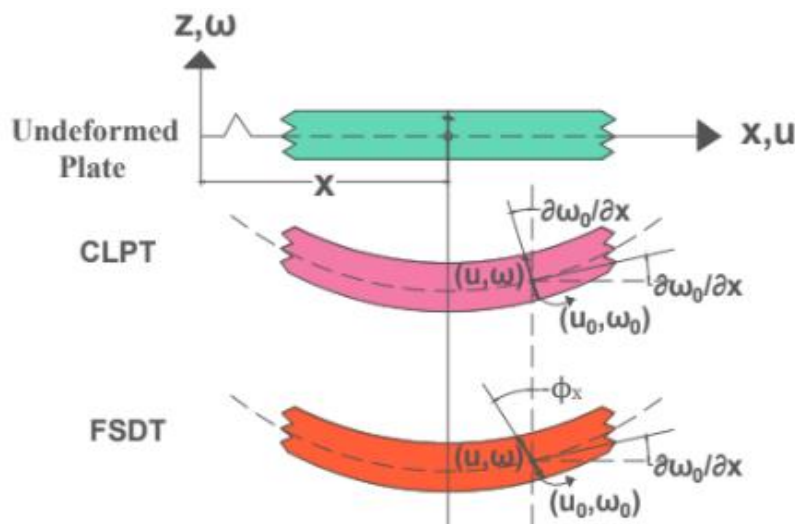


Figure 10 . The positive coordinate directions, stress resultants, and kinematic deformation of an edge in CPT and FSDT

Structural theories can be developed by expanding the displacements in a power series of the transverse coordinates. This can be done using simple polynomials or with orthogonal polynomials such as Legendre, Hermite or Chebyshev polynomials. A simple expansion without any further restriction leads to what are called unconstrained theories. Basic assumptions on the kinematics of the deformation or other considerations are usually made to reduce the number of variables to be determined while providing accurate solutions. This section presents an overview of polynomial theories for plates

that include the classical plate theory (CPT) and the first order shear deformation theory (FSDT).

1.4.1 Classical Plate Theory (CPT):-

The classical plate theory (CPT) is also known by the Kirchhoff-Love theory. It was developed by Love and Darwin in 1888 [8] using assumptions proposed by Kirchhoff [9] in 1850. This theory is usually called the Classical plate theory (CPT) and its main assumption is that a line segment normal to the mid plane remains straight and remains perpendicular to the mid-surface after deformation. This section will review the three basic assumptions of that theory and how they lead to a particular choice of the displacement field. This is followed by the procedure generally followed to generate the constitutive equations, the equations of motion, and the boundary conditions for any theory which will not need to be repeated.

1.4.1.1 Kinematics of the CPT:-

Starting with the polynomial expansion of the displacements, the transverse shear strains and the transverse normal strains are:

$$\varepsilon_{xz} = u_1 + w_{0,x} + z(2u_2 + w_{1,x}) + z^2(3u_3 + w_{2,x}) + \dots + z^n[(n+1)u_{n+1} + w_{n,x}] \quad (1.1a)$$

$$\varepsilon_{yz} = v_1 + w_{0,y} + z(2v_2 + w_{1,y}) + z^2(3v_3 + w_{2,y}) + \dots + z^n[(n+1)v_{n+1} + w_{n,y}] \quad (1.1b)$$

$$\varepsilon_{zz} = w_1 + 2zw_2 + 3z^2w_3 + \dots + nZ^{n-1}w_n \quad (1.1c)$$

The development of the classical (Kirchhoff-Love) plate theory is based on three basic assumptions:

1. The thickness of the plate does not change during a deformation, i.e. inextensibility in the transverse direction ($\varepsilon_{zz} = 0$). Then, **Eq. 1.1c** indicates that the higher order terms in the polynomial expansion for w are zero for $w = w_0$.

2. Line segments perpendicular to the reference surface remains straight so the two transverse shear strains are independent of z , i.e., $u_i = 0$ and $v_i = 0$ for $i \geq 2$.

3. Line segments normal to the reference surface remain perpendicular to that surface. This implies that transverse shear strains are neglected, so $\varepsilon_{xz} = 0$ and $\varepsilon_{yz} = 0$. From **Eq. 1.1-a, b** we find that $u_1 + w_{0,x} = 0$ and $v_1 + w_{0,y} = 0$.

The deformation of the plate is described by only three variables u_0, v_0, w_0 , so

$$u = u_0 - zw_{0,x}, \quad v = v_0 - zw_{0,y}, \quad w = w_0 \quad (1.2)$$

The strain-displacement relations are

$$\begin{Bmatrix} \varepsilon_{xx} \\ \varepsilon_{yy} \\ \varepsilon_{xy} \end{Bmatrix} = \begin{Bmatrix} u_{0,x} \\ v_{0,y} \\ u_{0,y} + v_{0,x} \end{Bmatrix} + z \begin{Bmatrix} -w_{0,xx} \\ -w_{0,yy} \\ -2w_{0,xy} \end{Bmatrix} \quad (1.3)$$

where, the first bracket on the right-hand side $\{\varepsilon_0\}$ contains the strains of the reference surface. The second curly bracket gives the plate curvatures $\{k\}$.

Above **Eq. 1.3** can be written as:

$$\{\varepsilon\} = \{\varepsilon_0\} + z\{k\} \quad (1.4)$$

1.4.1.2 Remarks on the Classical Plate Theory

Reflecting on the assumptions of the theory, a simple beam example will show that this theory is valid when the length of the beam is large compare to the radius of gyration of its cross-section. Otherwise, shear deformations should be considered. Then we show that the shear stress follows a parabolic distribution through the thickness and that line segments perpendicular to the reference surface do not remain straight contrary to the second assumption of

the CPT. Because of Poisson's effect, some extension occurs in the transverse direction.

The third assumption in the development of the theory is that deformations due to transverse shear are negligible. To get some insight into the validity of this assumption, consider the bending of a simple homogeneous cantilever beam loaded by a concentrated load P at $x=0$ and clamped at $x=L$. the bending deflection w_b is related to the bending moment by $M=EI w_{b,xx}$ while the shear deflection w_s is related to the shear force V by $V = -GAw_{s,x}$. for this example, the tip deflections are $w_b = PL^3 / (3EI)$ and $w_s = PL / GkA$ where k is the shear correction factor. The ratio of these two deflections can be written as:

$$\frac{w_s}{w_b} = 3 \frac{E}{G} \frac{I}{kA} \frac{1}{L^2} = 3 \frac{E}{G} \frac{r^2}{L^2}$$

where $r = \sqrt{I/kA}$ is the radius of gyration of the beam effective cross-section. For isotropic materials $E/G=2(1+\nu)$. For a Poisson ratio of 0.3, $w_s / w_b < 0.01$ when $L > 27.9 r$. It is often said that the Bernoulli-Euler beam theory is valid for long beams so the present result gives an indication of what is meant by that statement. $E/G=2.6$ for an isotropic material with $\mu = 0.3$ but for composite materials the E_1/G_{12} ratio is usually much greater than that so that the effect of shear deformation is much greater. For example if $E/G=20$, $w_s / w_b < 0.01$ when $L > 77.5 r$. This example provides the motivation for developing plate theories that account for shear deformations. It is generally recognized that the classical plate theory can be used only for thin plates. This example shows that how thin it needs to be depends on the elastic properties of the material.

In the static case, the theory of elasticity indicates that during the cylindrical bending of a plate in the xz -plane, equilibrium in the x -direction is governed by $\sigma_{xx,x} + \sigma_{xz,z} = 0$. Since the CPT predicts that, for a homogeneous

beam, σ_{xx} varies linearly through the thickness, this equation indicates that the transverse shear stress σ_{xz} should follow a parabolic distribution through the thickness. Usually the shear stress is zero on the top and bottom surfaces so $\sigma_{xz} = \tau_x (1 - \frac{4z^2}{h^2})$. We find that the magnitude of the shear stress $\tau_x = \frac{3Q_x}{2}$. With the transverse shear $\varepsilon_{xz} = \frac{3Q_x}{2G} (1 - \frac{4z^2}{h^2})$, the displacement in the x-direction is of the form $u = u_0 - zw_{0,x} + \frac{3Q_x}{2G} z (1 - \frac{4z^2}{h^2})$.

The previous discussion is based on the assumption that the material is homogeneous. For a multilayer structure, the expressions given above for σ_{xz} and u no longer apply. The shear stress still varies quadratically in each layer but is described by a different expression in each layer. In bending, the classical plate theory predicts that $\varepsilon_{xx} = -zw_{0,xx}$ and $\varepsilon_{yy} = -zw_{0,yy}$. Because of the Poisson effect, the strain in the transverse direction is $\varepsilon_{zz} = -\nu(\varepsilon_{xx} + \varepsilon_{yy}) = \nu z(w_{0,xx} + w_{0,yy})$. Therefore, in addition to w_0 , the transverse displacement of the reference surface, the transverse displacement should include a quadratic term so $w = w_0 + \nu(z^2/2)(w_{0,xx} + w_{0,yy})$. Under biaxial tension, the in plane normal strains are constant through the thickness. From **Eq. 1.3** $\varepsilon_{xx} = u_{0,x}$ and $\varepsilon_{yy} = v_{0,y}$. Then, due to Poisson's effect, $\varepsilon_{zz} = -\nu(u_{0,x} + v_{0,y})$. This suggests that the transverse displacement should vary linearly through the thickness. Accounting for both types of Poisson's effects requires that $w = w_0 + zw_1 + z^2w_2$.

This discussion pointed out areas for improvement in the development of accurate theories. The first issue is to account for the effect of shear deformation and to accurately predict the shear stress distribution through the thickness.

1.4.2 First Order Shear Deformation Theory (FSDT)

The Mindlin-Reissner theory of plates, also referred to as the First order Shear Deformation Theory (FSDT), is an extension of Kirchhoff–Love plate theory that takes into account shear deformations through the thickness of a plate in an average sense. It was proposed by Reissner [10] and by MINDLIN, 1951[11]. The main difference with the classical plate theory is the third assumption in that theory. In FSDT, the normal to the reference surface remains inextensible and straight but is no longer assumed to remain perpendicular to the mid-surface after deformation. As a result, transverse shear strains (or stresses) are constant through the thickness. This implies that the variables u_1 and v_1 representing the rotations of the normal to the reference surface are now independent of $w_{0,x}$ and $w_{0,y}$, the rotations of that reference surface.

1.4.2.1 Kinematics of the FSDT:

With this theory, the kinematics of the deformation depends on five variables: u_0, v_0, u_1, v_1, w_0 . To use the notation generally adopted in the literature we now use $u_1 = \varphi_x$, $v_1 = \varphi_y$. The kinematics of the deformation of the FSDT is given by:

$$u = u_0 + z\varphi_x, v = v_0 + z\varphi_y, w = w_0 \quad (1.5)$$

and $w = w_0$. The strain displacements are also given by **Eq. 1.4**, but the curvatures are now given by:

$$\{k\} = \begin{Bmatrix} \varphi_{x,x} \\ \varphi_{y,y} \\ \varphi_{x,x} + \varphi_{y,y} \end{Bmatrix} \quad (1.6)$$

The transverse shear strains are

$$\begin{Bmatrix} \varepsilon_{yz} \\ \varepsilon_{xz} \end{Bmatrix} = \begin{Bmatrix} \varphi_y + w_{0,y} \\ \varphi_x + w_{0,x} \end{Bmatrix} \quad (1.7)$$

Whitney [12] first applied FSDT to the stress analysis of thick laminated composite and sandwich plates and showed how to determine the shear correction factors. For isotropic plates, Reissner [10] obtained the value $5/6$

1.5 Differential Quadrature Method (DQM)

It is well-known that difficulties in applying the analytical methods arise when complex geometries, patch loading, local elastic supports, mixed boundary conditions and other discontinuities are taken into account.

Thus, numerical approaches are mandatory to use. One of the numerical solution technique is the differential quadrature method(DQM) developed by Bellman and Casti, 1971[13]. It is usually used for solving ordinary and partial differential equations. As an analogous extension of the quadrature for integrals, it can be essentially expressed as the values of the derivatives at each grid point as weighted linear sums approximately of the function values at all grid points within the domain under consideration. It has the potential to serve as an alternative for finite element and finite difference methods, which are computationally inefficient and time consuming conventional numerical solution techniques.

The differential quadrature method is conceptually simple, and the implementation is straightforward. It has been recognized that the differential quadrature method has the capability of producing highly accurate solutions with minimal computational effort when the method is applied to problems with globally smooth solutions.

Up until now, DQM has been used to solve boundary-value problems in a great measure in various fields of science and engineering, notably structural mechanics [14]–[17], transport process [18] , dynamic systems [19]–[21] and calculation of transmission line transient response.

Using the Differential Quadrature Method (DQM), natural frequencies of FG curved panel subjected in a thermal environment were determined by solving the governing differential equation [22]. Malekzadeh and Ghaedsharaf, 2014[23] applied a layerwise-differential quadrature method (LW-DQM) in thickness direction of the laminated cylindrical panel having continuously varying material through the thickness and applied DQM in the axial direction of cylinder. Zahedinejad et al., 2010[24] used differential quadrature method (DQM) to discretize the governing equations efficiently under various related boundary conditions in free vibration analysis of thick FG curved panels having properties variation of material along the thickness based on power-law distribution and exponential distribution individually. Farid et al., 2010[25] used the differential quadrature method(DQM) in the FG curved panel's thickness direction with varying temperatures to discretize the governing equations.

1.6 Organization of the Report

The thesis is divided into six chapters. The first chapter gives a basic introduction to the types of plate material, Functionally Graded Materials, the Plate theories and the method of solution employed (Differential Quadrature Method). The second chapter presents a literature survey of the solution methodologies employed worldwide till date. The third chapter discusses the mathematical formulation of the vibration problem of circular FGM using DQM. The fourth comprises of the solution methodology for the problem. The fifth chapter discusses the free vibration analysis and the results obtained from the parametric study. The sixth and the final chapter concludes the project and summarizes the parametric studies conducted.

2. Literature Review

Plates and shells of various geometries are widely used in modern engineering structures which has drawn the attention of researchers throughout the world to study the static/dynamic behavior of structures with a great accuracy using analytical/numerical methods and different theories. Venkateswara Rao, 1976 [26] presented a finite element formulation for the large amplitude free oscillations of beams and orthotropic circular plates. The proposed formulation by the author did not need the knowledge of longitudinal/in-plane forces developed due to large displacements and thus avoided the use of corresponding geometric stiffness matrices. Raju and Rao, 1976 [27] formulated the problem by employing the finite element method considering both simply supported and clamped plates. The predicted results indicated that the influence of geometric non-linearity was found to be greater when the effects of shear deformation and rotatory inertia were included than when they were neglected. Rao and Raju, 1980 [28] evaluated the effects of elastically restrained edges (against rotation) on the large amplitude vibrations of simply supported and clamped orthotropic circular plates by using finite element formulation. WANG et al., 1995[29] and Romanelli et al., 1998[30] solved the free vibrations of annular plates using the differential quadrature method (DQM) applying four boundary conditions, two for each outer and inner edge, respectively. GU and WANG, 1997[31] employed three (two for the outer edge and one for the center) conditions for solid circular plates and obtained some results using the DQM. Axisymmetric free vibrations of moderately thick circular plates described by the linear shear-deformation Mindlin theory are analyzed by the differential quadrature (DQ) method by Liew et al., 1997[32]. The generalized differential quadrature rule proposed by Wu and Liu, 2001[33] is applied here to the free vibration analyses of solid circular plates with radially varying thickness and elastic restraints. The thickness varies radially in

exponential and linear form. Wang et al., 2002[34] used meshless approach for the flexural, free vibration and buckling analysis of laminated composite plates employing the first-order shear deformation theory (FSDT). Najafizadeh and Eslami, 2002[35] presented the buckling analysis of radially loaded solid circular plate made of functionally graded material. The edge of the plate is either simply supported or clamped and the plate is assumed to be geometrically perfect. The equations are based on Love–Kirchhoff hypothesis and the Sander's non-linear strain-displacement relation. The free vibration of solid circular plates has been studied using the generalized differential quadrature rule (GDQR) by Wu et al., 2002[36]. Liew et al., 2003[37] adopted the first-order shear deformation theory in the moving least squares differential quadrature (MLSDQ) procedure for predicting the free vibration behavior of moderately thick symmetrically laminated composite plates. Haterbouch and Benamar, 2005 [38] studied nonlinear free axisymmetric vibration of simply supported isotropic circular plates by using the energy method and a multimode approach. The limit of validity of the single-mode approach is also investigated. The only problem with the single-mode approach was found that it was not able to predict the deformation of the mode shape of the simply supported immovable circular plate, which induces over-estimated maximum bending stresses. The authors concluded that the single-mode approach is suitable for engineering design of simply supported immovable circular plates undergoing vibrations of finite amplitudes up to once their thickness. Vel and Batra, 2004 [39] presented a three-dimensional exact solution for free and forced vibrations of simply supported functionally graded rectangular plates. BATRA and JIN, 2005[40] used the first-order shear deformation theory (FSDT) together with the finite element method (FEM) to study free vibrations of a functionally graded (FG) anisotropic rectangular plate with the objective of maximizing one of its first five natural frequencies. Zenkour, 2006 [41] investigated the static response for a simply supported functionally graded rectangular plate subjected to a

transverse uniform load. The generalized shear deformation theory obtained by the author in other recent papers is used. Gupta et al., 2006 [5] employed the differential quadrature method (DQM) to examine the effect of the non-homogeneity of the material on the natural frequencies of circular plates of quadratically varying thickness on the basis of classical plate theory. Ebrahimi and Rastgo, 2008 [43] analytically investigated the free vibration behavior of thin circular functionally graded (FG) plates integrated with two uniformly distributed actuator layers made of piezoelectric (PZT4) material based on the classical plate theory (CPT). The differential equations of motion were solved analytically for clamped edge boundary condition of the plate. The detailed emphasis was placed on investigating the effect of varying the gradient index of FG plate on the free vibration characteristics of the structure. Yalcin et al., 2009[44] analyses the free vibrations of circular thin plates for simply supported, clamped and free boundary conditions. The solution method used is differential transform method (DTM), which is a semi-numerical–analytical solution technique that can be applied to various types of differential equations. Carrera et al., 2010[45] investigates the static response problem of multilayered plates and shells embedding functionally graded material (FGM) layers. Singha et al., 2011[46] investigated the nonlinear behaviors of functionally graded material (FGM) plates under transverse distributed load using a high precision plate bending finite element and developed formulation based on the first-order shear deformation theory considering the physical/exact neutral surface position. Kiani et al., 2012 [47] investigated the static, dynamic, and free vibration analysis of a functionally graded material (FGM) doubly curved panel. Castellazzi et al., 2013[48] presented the nodal integrated plate element (NIPE) formulation for the analysis of functionally graded plates based on the first-order shear deformation theory. Thai and Choi, 2013 [49] formulated analytical solutions for bending, buckling, and vibration analyses of thick rectangular plates with various boundary conditions using two variable refined plate theory.

Duan et al., 2014 [50] presented novel formulation by using the discrete singular convolution (DSC) for free vibration analysis of circular thin plates with uniform and stepped thickness. The proposed DSC circular and annular plate elements are used for obtaining frequencies of uniform/stepped circular thin plates or annular thin plates with different boundary conditions. Farahani et al., 2015[51] extended the radial point interpolation method (RPIM) to the elasto-static analysis of circular plates. Wang et al., 2016 [52] presented a unified method for the vibration analysis of the plates mentioned above with general boundary conditions based on the first-order shear deformation theory and Ritz procedure. The auxiliary functions were introduced to eliminate all the relevant discontinuities with the displacement and its derivatives at the boundaries and to accelerate the convergence of series representations. Żur, 2018[53] employed the quasi-Green's function to solve the boundary value problem of the free vibrations of functionally graded circular plates with clamped, free and simply supported edges. The analysis and numerical results FG circular plates elastically supported on a concentric ring are presented on the basis of the classical plate theory. Khare and Mittal, 2019 [54] analysed free vibration results of symmetrically laminated circular and annular plates having elastic edge constraints with each layer having cylindrical/polar orthotropy utilizing a Differential Quadrature Methodology (DQM) for spatial discretization. Roshanbakhsh et al., 2020 [55] presented a simple and effective analytical method based on displacement potential functions for solving the 3D free vibration problem of the functionally graded circular plates with surface boundary conditions consisting of a transversely isotropic linearly elastic material. Wattanasakulpong et al., 2012[56] showed the importance of considering porosity factor in the design and analysis of FGM plates. The pores in the microstructures of such structural materials are accounted via local density of the material.

The vibration characteristics of longitudinally travelling porous FGM plates was first investigated by Wang et al., 2017[57]. Kiran et al., 2018[58] studied the influence of porosity on structural behavior of skew FG MEE plate. Ebrahimi et al., 2017[59] analysed the vibration characteristics of MEE heterogeneous porous material plates resting on elastic foundations. Barati et al., 2017 [60] employed a four variable refined plate theory to calculate the electro-mechanical vibration of smart piezoelectric FG plates with porosities. Although the manufacturing techniques have improved significantly, the porosity is a common defect often observed in FGMs. Hence, it is intended to develop a suitable model to study the behavior of FGM plates accounting the inherent porosity in the material. Hence, in this project, the differential quadrature method is utilized to evaluate the free vibration and static characteristics of circular porous FGM plate for different porosity models is considered for evaluation. The effect of different porosity distribution, porosity volume index, and gradient index affecting the structural behavior of porous FGM plate is extensively investigated. Further, the effect of thickness ratio, aspect ratio, and boundary condition is also studied.

3. Mathematical Formulation

3.1 Introduction

The aim of this chapter is to develop the governing differential equations of equilibrium and corresponding domain boundary conditions. The studies on elastic behavior of FGM plates started with Classical laminate plate theory, was initiated by Kirchhoff. The Kirchhoff assumption amounts to neglecting both transverse shear and a transverse normal strain effect, i.e., deformation is due entirely to bending. To consider the effects of the transverse shear strain first-order shear deformation theories (FSDT) have been attempted. The first order shear deformation theory assumes the distribution of transverse shear strain to be constant through the plate thickness. It is thus the simplest approximation and has been found to be a good compromise between computational accuracy and efficiency.

3.2 Plate description

Consider a porous FGM circular plate of radius r and thickness h with varying properties through the thickness which is shown in **Figure 11**. R_0 and R_i are external and internal radius respectively. The coordinate axis is taken on the middle plane of the plate. With z showing the variable across the plate cross section. The effective materials properties of the PFGM plate are uniform across the thickness direction based on the modified power-law in the Voigt model. The five types of porosity distributions in PFGM circular plate along the thickness direction are as follows

PD-1: Uniform porosity distribution, [61]

$$P(z) = [P_c - P_m] \left(\frac{2z+h}{2h} \right)^n + P_m - \frac{\text{por}}{2} (P_c + P_m) \quad (3.1)$$

PD-2: O-shape centralized porosity distribution, [61]

$$P(z) = [P_c - P_m] \left(\frac{2z+h}{2h} \right)^n + P_m - \frac{\text{por}}{2} (P_c + P_m) \left(1 - \frac{2|z|}{h} \right) \quad (3.2)$$

PD-3: X-shape centralized porosity distribution, [61]

$$P(z) = [P_c - P_m] \left(\frac{2z+h}{2h} \right)^n + E_m - \frac{\text{por}}{2} (P_c + P_m) \left(\frac{2|z|}{h} \right) \quad (3.3)$$

PD-4: V-shape porosity distribution, [61]

$$P(z) = [P_c - P_m] \left(\frac{2z+h}{2h} \right)^n + P_m - \frac{\text{por}}{2} (P_c + P_m) \left(1 + \frac{2|z|}{h} \right) \quad (3.4)$$

PD-5: Logarithmic distribution porosity distribution, [62]

$$P(z) = P_c - P_m \left(\frac{2z+h}{2h} \right)^n + P_m - \log \left(1 + \frac{\text{por}}{2} \right) P_c + P_m \left(1 - 2 \frac{|z|}{h} \right) \quad (3.5)$$

where, the subscripts c and m refer to ceramics and metal respectively and ‘por’ is the porosity index, m is the grading index and P is the material property which includes (Young's modulus E, Poisson's ratio μ , and mass density ρ) .

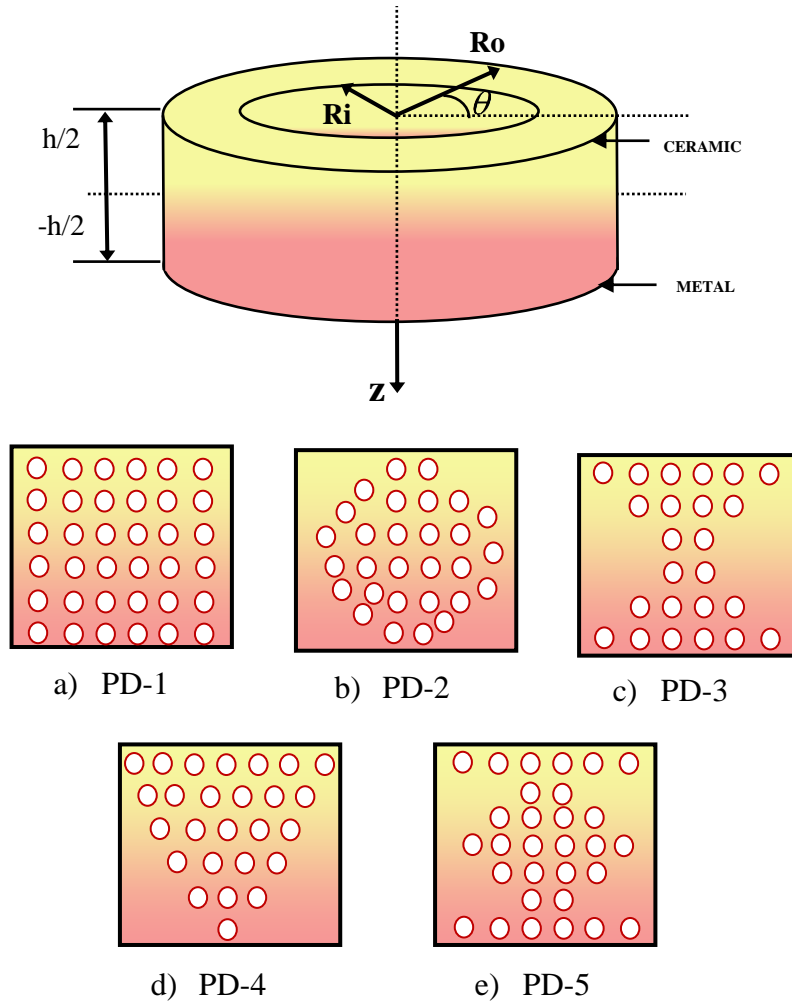


Figure 11. The geometry of the circular FGM plate with five type of porosity distribution models.

3.3 Strain displacement relations

The assumed displacements based on first order shear deformation theory of a point in the circular plate are defined as:

$$\begin{Bmatrix} u(r, \theta, z, t) \\ v(r, \theta, z, t) \\ w(r, \theta, z, t) \end{Bmatrix} = \begin{Bmatrix} u_0(r, \theta, z, t) \\ v_0(r, \theta, z, t) \\ w_0(r, \theta, z, t) \end{Bmatrix} + z \begin{Bmatrix} \phi_r(r, \theta, t) \\ \phi_\theta(r, \theta, t) \\ 0 \end{Bmatrix} \quad (3.6)$$

Where u , v and w represent the unknown displacements of the plate middle surface in the r , θ and z direction, respectively, and ϕ_r , ϕ_θ represent the transverse normal rotations of rz and θz planes. Besides, t is the time variable.

The strains of FGM circular plate can be written as:

$$\begin{Bmatrix} \varepsilon_r \\ \varepsilon_\theta \\ \gamma_{\theta z} \\ \gamma_{rz} \\ \gamma_{r\theta} \end{Bmatrix} = \begin{Bmatrix} \varepsilon_r^0 \\ \varepsilon_\theta^0 \\ \gamma_{\theta z} \\ \gamma_{rz} \\ \gamma_{r\theta}^0 \end{Bmatrix} + z \begin{Bmatrix} \kappa_r^0 \\ \kappa_\theta^0 \\ 0 \\ 0 \\ \kappa_{r\theta}^0 \end{Bmatrix} = \begin{Bmatrix} \frac{\partial u}{\partial r} \\ \frac{1}{r} \left(u + \frac{\partial v}{\partial \theta} \right) \\ \phi_\theta + \frac{1}{r} \frac{\partial w}{\partial \theta} \\ \phi_r + \frac{\partial w}{\partial r} \\ \frac{1}{r} \left(\frac{\partial u}{\partial \theta} - v \right) + \frac{\partial v}{\partial r} \end{Bmatrix} + z \begin{Bmatrix} \frac{\partial \phi_r}{\partial r} \\ \frac{1}{r} \left(\phi_r + \frac{\partial \phi_\theta}{\partial \theta} \right) \\ 0 \\ 0 \\ \frac{1}{r} \left(\frac{\partial \phi_r}{\partial \theta} - \phi_\theta \right) + \frac{\partial \phi_\theta}{\partial r} \end{Bmatrix} \quad (3.7)$$

Where, ε_r^0 and ε_θ^0 are the normal strains; $\gamma_{r\theta}^0$ denote the shear strains; γ_{rz} and $\gamma_{\theta z}$ represent the transverse shear strains; κ_r^0 , κ_θ^0 and $\kappa_{r\theta}^0$ express the curvature changes.

3.4 Constitutive equations

The stress-strain relation using Hook's law with respect to the structural axis system for the FGM circular plate can be expressed as

$$\begin{Bmatrix} \sigma_r \\ \sigma_\theta \\ \sigma_{r\theta} \end{Bmatrix} = \begin{bmatrix} Q_{11} & Q_{12} & 0 \\ Q_{12} & Q_{22} & 0 \\ 0 & 0 & Q_{66} \end{bmatrix} \begin{Bmatrix} \varepsilon_r \\ \varepsilon_\theta \\ \gamma_{r\theta} \end{Bmatrix} \quad (3.8)$$

$$\begin{Bmatrix} \sigma_{\theta z} \\ \sigma_{rz} \end{Bmatrix} = \begin{bmatrix} Q_{44} & Q_{45} \\ Q_{45} & Q_{55} \end{bmatrix} \begin{Bmatrix} \gamma_{rz} \\ \gamma_{\theta z} \end{Bmatrix} \quad (3.9)$$

By taking strain-displacement relations and stress-strain relations, applying integration by parts and the fundamental lemma of variational calculus and the governing differential equations of the plate are obtained as:

$$\frac{\partial N_r}{\partial r} + \frac{1}{r} \left(\frac{\partial N_r}{\partial \theta} + N_r - N_\theta \right) = I_0 \frac{\partial^2 u}{\partial t^2} + I_1 \frac{\partial^2 \phi_r}{\partial t^2} \quad (3.10)$$

$$\frac{\partial N_{r\theta}}{\partial r} + \frac{1}{r} \left(\frac{\partial N_\theta}{\partial \theta} + 2N_{r\theta} \right) = I_0 \frac{\partial^2 v}{\partial t^2} + I_1 \frac{\partial^2 \phi_\theta}{\partial t^2} \quad (3.11)$$

$$\frac{\partial Q_r}{\partial r} + \frac{1}{r} \left(\frac{\partial Q_\theta}{\partial \theta} + Q_r \right) = I_0 \frac{\partial^2 w}{\partial t^2} \quad (3.12)$$

$$\frac{\partial M_r}{\partial r} + \frac{1}{r} \left(\frac{\partial M_{r\theta}}{\partial \theta} + M_r - M_\theta \right) - Q_r = I_1 \frac{\partial^2 u}{\partial t^2} + I_2 \frac{\partial^2 \phi_r}{\partial t^2} \quad (3.13)$$

$$\frac{\partial M_{r\theta}}{\partial r} + \frac{1}{r} \left(\frac{\partial M_\theta}{\partial \theta} + 2M_{r\theta} \right) - Q_\theta = I_1 \frac{\partial^2 v}{\partial t^2} + I_2 \frac{\partial^2 \phi_\theta}{\partial t^2} \quad (3.14)$$

The forces and moments of a FGM circular plate can be obtained as below:

$$\begin{Bmatrix} N_r \\ N_\theta \\ N_{r\theta} \end{Bmatrix} = \begin{bmatrix} A_{11} & A_{12} & 0 \\ A_{12} & A_{22} & 0 \\ 0 & 0 & A_{66} \end{bmatrix} \begin{Bmatrix} \varepsilon_r^0 \\ \varepsilon_\theta^0 \\ \gamma_{\theta z} \end{Bmatrix} + \begin{bmatrix} A_{11} & A_{12} & 0 \\ A_{12} & A_{22} & 0 \\ 0 & 0 & A_{66} \end{bmatrix} \begin{Bmatrix} \kappa_r^0 \\ \kappa_\theta^0 \\ \kappa_{r\theta}^0 \end{Bmatrix} \quad (3.15)$$

$$\begin{Bmatrix} M_r \\ M_\theta \\ M_{r\theta} \end{Bmatrix} = \begin{bmatrix} B_{11} & B_{12} & 0 \\ B_{12} & B_{22} & 0 \\ 0 & 0 & B_{66} \end{bmatrix} \begin{Bmatrix} \varepsilon_r^0 \\ \varepsilon_\theta^0 \\ \gamma_{\theta z} \end{Bmatrix} + \begin{bmatrix} D_{11} & D_{12} & 0 \\ D_{12} & D_{22} & 0 \\ 0 & 0 & D_{66} \end{bmatrix} \begin{Bmatrix} \kappa_r^0 \\ \kappa_\theta^0 \\ \kappa_{r\theta}^0 \end{Bmatrix} \quad (3.16)$$

$$\begin{Bmatrix} Q_r \\ Q_\theta \end{Bmatrix} = \bar{k} \begin{Bmatrix} A_{44} & 0 \\ 0 & A_{55} \end{Bmatrix} \begin{Bmatrix} \gamma_{rz} \\ \gamma_{\theta z} \end{Bmatrix} \quad (3.17)$$

Where, $\bar{k}(=5/6)$ is the shear correction factor. The symbol A_{ij} , B_{ij} and D_{ij} are the extensional, coupling and bending stiffness of the plate respectively.

$$A_{ij} = \sum Q_{ij} (z_{h/2} - z_{-h/2}), \quad (i, j = 1, 2, 6). \quad (3.18)$$

$$A_{ij} = \bar{k} \sum Q_{ij} (z_{h/2} - z_{-h/2}), \quad (i, j = 4, 5) \quad (3.19)$$

$$B_{ij} = \frac{1}{2} \sum Q_{ij} (z_{h/2}^2 - z_{-h/2}^2), \quad (i, j = 1, 2, 6) \quad (3.20)$$

$$D_{ij} = \frac{1}{3} \sum Q_{ij} (z_{h/2}^3 - z_{-h/2}^3), \quad (i, j = 1, 2, 6) \quad (3.21)$$

The mass inertias of the plate I_i ($i = 0, 1, 2$) are defined as follows

$$I_i = \sum \int_{-\frac{h}{2}}^{\frac{h}{2}} \rho(1, z, z^2) dz \quad \text{and } (i = 0, 1, 2) \quad (3.22)$$

Where, ρ^k denotes the density of k^{th} layer.

In this work, the inertia component I_1 is taken as zero, due to symmetry in terms of mass density about the middle surface of laminated plate. However, presence of in-inertia is controlled by the parameter α_{uv} , by putting $\alpha_{uv} = 0$ or 1 in mathematical formulation.

4. Solution Methodology

The essence of the DQM relies on the idea that a derivative of a function with respect to a variable at any discrete point can be approximated as a weighted linear sum of the function values at all the discrete points chosen in the overall domain of that variable. The differential quadrature method is first employed to convert the differential equations into a set of linear algebraic equations. Then by solving the algebraic equations, solutions to the problem are obtained.

Supposing that there are N_x grid points in the x -direction and N_y in the y -direction with x_1, x_2, \dots, x_{N_x} and $y_1, y_2, y_3, \dots, y_{N_y}$ as the coordinates, the n^{th} -order partial derivative with respect to x , the m^{th} -order partial derivative of $f(x, y)$ with respect to y and the $(n + m)^{\text{th}}$ -order partial derivative of $f(x, y)$ with respect to both x and y can be expressed discretely at the point (x_i, y_i) as [63] :

$$f_x^{(n)}(x_i, y_j) = \sum_{k=1}^{N_x} C_{ik}^{(n)} f(x_k, y_j); \quad n = 1, 2, \dots, N_x - 1 \quad (4.1)$$

$$f_y^{(m)}(x_i, y_j) = \sum_{k=1}^{N_y} \bar{C}_{ik}^m f(x_i, y_k); \quad m = 1, 2, \dots, N_y - 1 \quad (4.2)$$

$$f_{xy}^{(n+m)}(x_i, y_j) = \sum_{k=1}^{N_x} C_{ik}^{(n)} \sum_{l=1}^{N_y} \bar{C}_{il}^m f(x_k, y_l); \quad \text{for } i = 1, 2, \dots, N_x, j = 1, 2, \dots, N_y \quad (4.3)$$

where $C_{ij}^{(n)}$ and \bar{C}_{ij}^m are weighting coefficients associated with n^{th} -order partial derivative of $f(x, y)$ with respect to x at the discrete point x_i and m^{th} -order derivative with respect to y at y_i , respectively.

Using the generalised and simplified DQ method, the weighting coefficients in above equation, i.e. $C_{ij}^{(n)}$ and \bar{C}_{ij}^m , can be determined as follows :

$$C_{ij}^{(1)} = \frac{M^{(1)}(x_i)}{(x_i - x_j)M^{(1)}(x_j)}; \quad \text{for } i, j = 1, 2, \dots, N_x, \text{ but } j \neq i, \quad (4.4)$$

$$\bar{C}_{ij}^{(1)} = \frac{P^{(1)}(y_i)}{(y_i - y_j)M^{(1)}(y_j)}; \quad \text{for } i, j = 1, 2, \dots, N_y, \text{ but } j \neq i, \quad (4.5)$$

Where

$$M^{(1)}(x_i) = \prod_{j=1, j \neq i}^{N_x} (x_i - x_j), \quad (4.6)$$

$$P^{(1)}(y_i) = \prod_{j=1, j \neq i}^{N_y} (y_i - y_j), \quad (4.7)$$

And

$$C_{ij}^{(n)} = n \left(C_{ii}^{(n-1)} C_{ij}^{(1)} - \frac{C_{ij}^{(n-1)}}{x_i - x_j} \right) \quad (4.8)$$

for $i, j = 1, 2, \dots, N_x$, but $j \neq i$; and $n = 2, 3, \dots, N_x - 1$

$$\bar{C}_{ij}^{(m)} = m \left(\bar{C}_{ii}^{(m-1)} \bar{C}_{ij}^{(1)} - \frac{\bar{C}_{ij}^{(m-1)}}{y_i - y_j} \right) \quad (4.9)$$

for $i, j = 1, 2, \dots, N_y$, but $j \neq i$; and $m = 2, 3, \dots, N_y - 1$

$$C_{ii}^{(n)} = - \sum_{j=1, j \neq i}^{N_x} C_{ij}^{(n)}; \quad i, j = 1, 2, \dots, N_x, \quad n = 1, 2, \dots, N_x - 1 \quad (4.10)$$

$$\bar{C}_{ii}^{(m)} = - \sum_{j=1, j \neq i}^{N_y} \bar{C}_{ij}^{(m)}; \quad i, j = 1, 2, \dots, N_y, \quad n = 1, 2, \dots, N_y - 1 \quad (4.11)$$

Once the functional values at all grid points are calculated, the value at any point could be readily obtained in terms of the polynomial approximation: Most of the previous works have reported of weighting co-efficients using relation given in equation. However, in this work method followed is as follow:

The 1st spatial derivatives of a general function $\varphi_r(r)$ at the $(i)^{th}$ point in a 1-dimensional domain (having M divisions in that r -direction) can be approximated using the DQM as:

$$\left. \frac{\partial \varphi_r}{\partial r} \right|_i = \sum_{k=1}^M C_{rik}^{(1)} \Psi_{rk} \quad (4.12)$$

where,

- $C_{rik}^{(1)}$ is the weighting coefficient of the value of φ_r at the k^{th} point for the 1st order derivative with respect to r calculated at the i^{th} point.
- Ψ_{rk} is the value of φ_r at the k^{th} point in the 1-dimensional domain.

In this study, a cosine law is used for generation of grid points.

$$r_i = b + \frac{(a-b)}{2} \left\{ 1 - \cos \left[\frac{(i-1)\pi}{M-1} \right] \right\} \quad \text{for } i = 1, 2, \dots, M \quad (4.13)$$

where, a and b are the outer and inner radii of the circular and annular plate.

Let Ψ_r be an M -dimensional vector having the nodal values of φ_r in the one-dimensional domain as follows,

$$\Psi_r = \left\{ \begin{array}{c} \Psi_{r1} \\ \Psi_{r2} \\ \dots \\ \dots \\ \dots \\ \Psi_{r(M-1)} \\ \Psi_{rM} \end{array} \right\} \quad (4.14)$$

and $C_r^{(1)}$ be an $M \times M$ matrix having the coefficients $C_{rik}^{(1)}$ as follows,

$$C_r^{(1)} = [C_{rik}^{(1)}] \quad (4.15)$$

Hence, $(i, k)^{th}$ element of the matrix $C_r^{(1)}$ gives the weighting coefficient of Ψ_{rk} for obtaining the 1^{st} derivative of φ_r at the i^{th} point as defined in the **Eq. (4.15)**. Thus, if $\Psi_r^{(1)}$ is an M -dimensional vector having the nodal values of 1^{st} derivative of φ_r , then, the following matrix relation holds,

$$\Psi_r^{(1)} = C_r^{(1)} \Psi_r \quad (4.16)$$

Or, in general, for the p^{th} order derivative,

$$\Psi_r^{(p)} = [C_r^{(1)}]^p \Psi_r \quad (4.17)$$

Similarly, if $\varphi_\theta(\theta)$ be a function of only θ , represented by N number of nodal values in a vector Ψ_θ , nodal values of its q^{th} degree derivative can be obtained with a similar $N \times N$ matrix $C_\theta^{(1)}$ having the coefficients $C_{\theta jl}^{(1)}$ as follows,

$$\Psi_\theta^{(q)} = [C_\theta^{(1)}]^q \Psi_\theta \quad (4.18)$$

The above procedure for 1-dimensional variables can easily be extended to 2-dimensional variables. The $M \times N$ nodal values of $(p, q)^{th}$ degree derivative of a 2-dimensional variable $\varphi_r(r, \theta)$ can be obtained as follows,

$$\Psi_{r\theta}^{(pq)} = [C_{2d\theta}^{(1)}]^q [C_{2dr}^{(1)}]^p \Psi_{r\theta} \quad (4.19)$$

Here,

$$\Psi_{r\theta} = \left\{ \begin{array}{c} \Psi_{r\theta 11} \\ \Psi_{r\theta 21} \\ \dots \\ \Psi_{r\theta ij} \\ \dots \\ \Psi_{r\theta (M-1)N} \\ \Psi_{r\theta MN} \end{array} \right\} \quad (4.20)$$

and, the 2-dimensional coefficient matrices $C_{2dr}^{(1)}$ and $C_{2d\theta}^{(1)}$ are defined in terms of the corresponding 1-dimensional matrices $C_r^{(1)}$ and $C_\theta^{(1)}$ (ref. **Eq. (4.15) and (4.18)**) as,

$$C_{2dr}^{(1)} = I_N \otimes C_r^{(1)} \quad (4.21)$$

$$C_{2d\theta}^{(1)} = C_r^{(1)} \otimes I_M \quad (4.22)$$

Here, \otimes is the Kronecker product, and, I_M and I_N are identity matrices of respective sizes. Similar to the equation 16, the grid point coordinates for the circumferential (*theta*) direction are generated using the following relation, for $i = 1, 2 \dots N$.

$$\theta_i = \frac{\theta}{2} \left\{ 1 - \cos \left[\frac{(i-1)\pi}{M-1} \right] \right\} \quad (4.23)$$

In the linear free vibration problem of a laminated plate, each of the five degrees of freedom at each of the nodes of the mesh can be assumed to be varying sinusoidally with respect to time, excluding the constrained degrees of freedom at the nodes located on boundary. Thus, for example, the displacement component w at the $(i,k)^{th}$ point is assumed as,

$$w_{ij} = W_{ij} \sin \omega t \quad (4.24)$$

In this way, the formulas given in equation (4.1- 4.3) are not needed.

5. Result and Discussion

5.1 Free Vibration Analysis of FGM Circular Plate

To establish the accuracy and effectiveness of the employed methodology, a convergence and comparison study is performed. Two types of PFGM are considered in the present analysis and depicted in **Table 1**. The fundamental frequency of a simply supported and clamp supported isotropic circular plate is tabulated in **Table 2** and **Table 3** respectively. The fundamental frequency parameter $\varpi = \omega h \sqrt{\rho/E}$ is considered with $R_0/h=10$. It is evident from the **Table 2** and **Table 3** that the frequency of all 6 modes is converging at (18x16) and are found to be in good agreement with the solutions by Mohammadi et al., 2013[64], Nguyen et al., 2015[65] and Thai et al., 2020[66]. The fundamental frequency of a C-C supported FGM-1 circular plate is plotted in **Figure 12**. The effective material properties and plate geometry is taken from Dong, 2008[67]. It is observed that the present results in good agreement with the three-dimensional solution using the Chebyshev–Ritz method Dong, 2008[67]. Based on the convergence results, it is observed that (18x16) mesh size is sufficient for the predicting free vibration results.

Table 1. Mechanical properties of metallic and ceramic materials considered

Types of Functionally graded material		Properties		
		E (GPa)	ρ (kg/m ³)	ν
PFGM-1	Metal (Al)	70	2702	0.3
	Ceramic (Al ₂ O ₃)	380	3800	0.3
PFGM-2	Metal (Al)	70	2702	0.3
	Ceramic (ZrO ₂)	151	3000	0.3

Table 2. Convergence and validation studies of fundamental frequency of isotropic circular plate. (Simply Supported plate)

Methods	Modes					
	I	II	III	IV	V	VI
Present (10x8)	4.8926	13.8548	25.4288	29.9457	49.2279	69.9271
Present (12x10)	4.9002	13.7605	25.6591	29.8811	41.3931	49.2661
Present (14x12)	4.9058	13.7124	25.4949	29.8410	40.4513	49.3601
Present (16x14)	4.9101	13.6541	25.5612	29.8145	39.8385	49.4721
Present (18x16)	4.9135	13.5868	25.5688	29.7956	39.9384	49.6281
Present (20x18)	4.9162	13.4950	25.5772	29.7813	39.9238	49.8776
Mohammadi et al., 2013 [64]	4.9345	13.8980	25.6130	29.7200	39.9570	48.4790
Nguyen et al., 2015 [65]	4.9304	13.8600	25.4820	29.5480	39.6560	48.0460
Nguyen et al., 2015 [65]	4.9304	13.8590	25.4800	29.5390	39.6330	48.0050
Thai et al., 2020 [66]	4.9304	13.8470	25.4410	29.5700	39.6010	48.1970

Table 3. Convergence and validation studies of fundamental frequency of isotropic circular plate. (Clamped plate)

Methods	Modes					
	I	II	III	IV	V	VI
Present (10x8)	10.2421	21.5615	34.7709	39.8025	61.2187	84.1527
Present (12x10)	10.2302	21.5224	34.9939	39.7729	52.7139	61.1506
Present (14x12)	10.2243	21.5355	34.7868	39.7585	51.5813	61.1721
Present (16x14)	10.2210	21.5477	34.8487	39.7507	50.8645	61.1990
Present (18x16)	10.2189	21.5733	34.8467	39.7460	50.9775	61.2455
Present (20x18)	10.2176	21.6231	34.8470	39.7430	50.9610	61.3302
Mohammadi et al., 2013 [64]	10.2160	21.2600	34.8770	39.7710	51.0300	60.8290
Nguyen et al., 2015 [65]	10.1850	21.1480	34.6130	39.3670	50.4950	60.0540
Nguyen et al., 2015 [65]	10.1840	21.1430	34.5890	39.3620	50.4390	59.9580
Thai et al., 2020 [66]	10.1840	21.1360	34.5580	39.4430	50.5630	60.4080

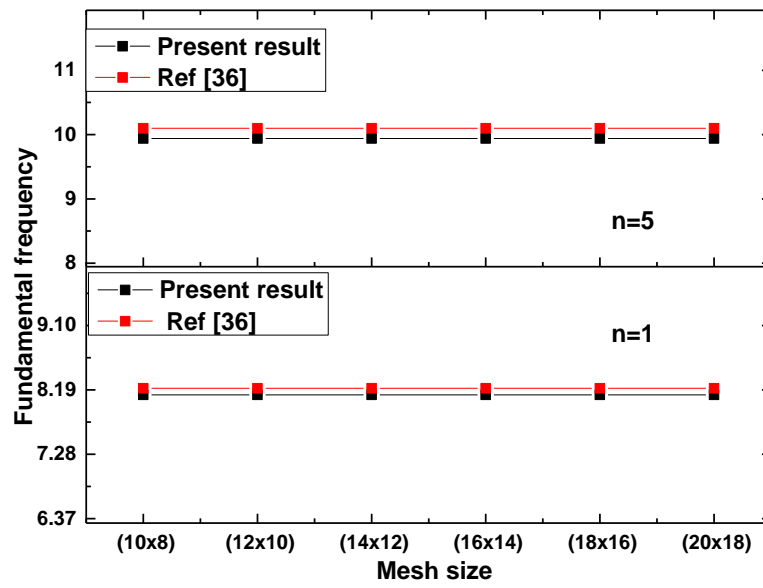


Figure 12. Convergence and comparison study of C-C PFGM-1 annular plate

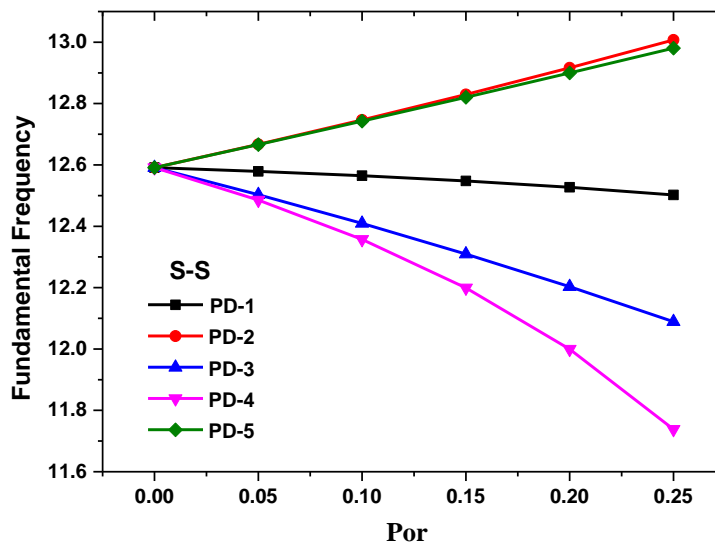


Figure 13. Influences of porosity index on fundamental frequency of PFGM-2 S-S circular plate with different porosity distribution type ($n=1$, $Ro=10$, $Ri=1$, $h=0.1$)

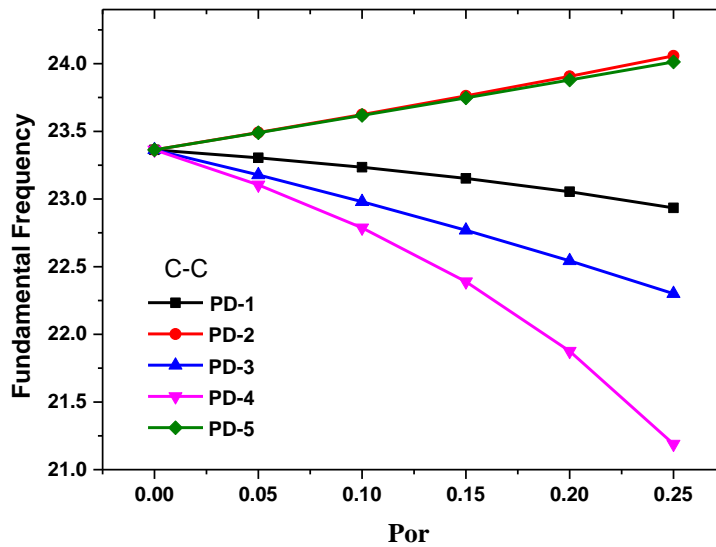


Figure 14. Influences of porosity index on fundamental frequency of PFGM-2 C-C circular plate with different porosity distribution type ($n=1$, $R_i/R_o=0.1$, $R_o/h=100$)

The influence of different types of porosity distribution on the fundamental frequency of PFGM annular plate vibration with S-S and C-C boundary conditions are represented in **Figure 13** and **Figure 14**. It is seen that by increasing the porosity index, the fundamental frequency start increasing for PD-2 and PD-5 and decreasing for PD-1, PD-3 and PD-4. The porosity index influence trend on the fundamental frequency is most pronounced in PD-4 and the least in PD-1. It is clearly seen that fundamental frequency for C-C boundary condition is greater than the S-S boundary condition but follow the same trend.

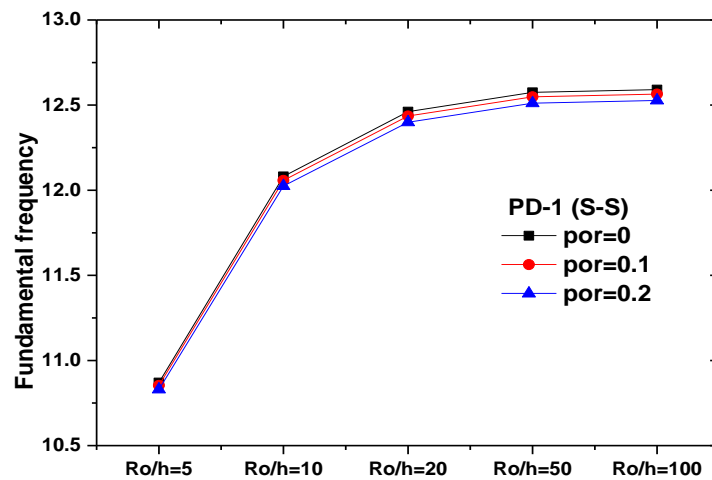
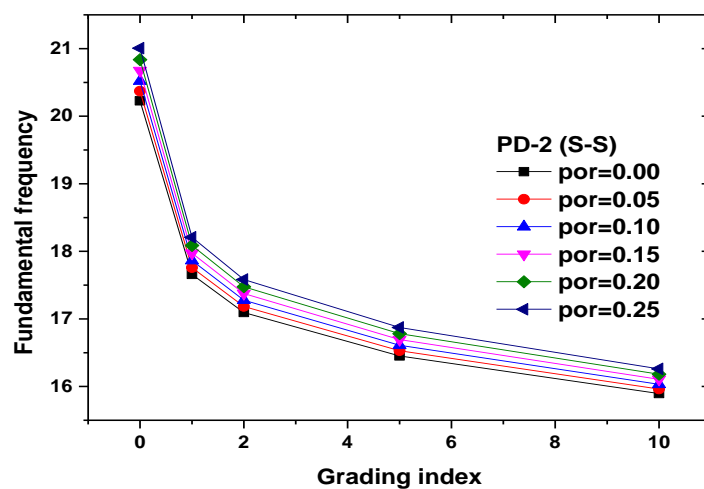


Figure 15. Influences of Ro/h ratio on fundamental frequency of PFGM-2 S-S circular plate with different porosity index ($n=1$, $Ro=10$, $Ri=1$, PD-1)

The effects of Ro/h ratio on the fundamental frequency of FGM-2 S-S annular plate under influence of PD-1 porosity model with different porosity index is plotted in **Figure 15**. It is clearly seen that with increase in porosity index, fundamental frequency decreases. Also, with increase in Ro/h ratio fundamental frequency increases and the effect of Ro/h ratio is negligible after



Ro/h=50.

Figure 16. Influences of grading index on fundamental frequency of PFGM-2 S-S circular plate with different porosity index ($Ro=10$, $Ri=3$, $Ro/h=10$, PD-2)

The effect of grading index on the fundamental natural frequency of PFGM-2 S-S annular plate with PD-2 is shown in **Figure 16**. It is observed that fundamental frequency increases with increase in porosity index and decreases with increase in grading index.

Table 4. Influence of Ri/Ro ratio on fundamental frequency of PFGM-2 S-S circular plate with different porosity index (Ro/h=20, PD-3, por=0.02, n=0.5)

Modes	Ri/Ro ratio					
	0	0.1	0.2	0.3	0.4	0.5
I	4.4657	12.9548	15.0487	18.8917	25.1402	35.6234
II	12.3506	14.9573	17.1800	20.8362	26.8546	37.1204
III	22.7522	23.0278	24.1988	26.8943	32.0825	41.6426
IV	26.3504	35.2932	35.5874	36.9969	40.8508	49.2140
V	35.3051	45.3632	49.7517	50.3104	52.7787	59.6203
VI	42.5310	49.4006	50.1058	50.6515	53.0902	59.8941

The effect of Ri/Ro on the first six frequencies of PFGM-2 circular plate with S-S and C-C boundary condition under influence of PD-3 is presented in **Table 4** and **Table 5** respectively. Geometric parameters (Ro/h=20, n=0.5, por=0.02) are considered for the study. It is observed that by increasing Ri/Ro ratio natural frequency increases. It is notable that fundamental frequency for clamp boundary condition is greater than the simply supported boundary condition but follow the same trend.

Table 5. Influence of Ri/Ro ratio on fundamental frequency of PFGM-2 C-C circular plate with different porosity index (Ro/h=20, PD-3, por=0.02, n=0.5)

Modes	Ri/Ro ratio					
	0	0.1	0.2	0.3	0.4	0.5
I	9.1074	23.8442	30.1402	39.2044	52.8686	74.8135
II	18.7729	25.1632	31.3717	40.2659	53.7693	75.5702
III	30.6618	31.9081	36.2441	44.0163	56.7548	77.9820
IV	34.9100	44.6118	46.2352	51.5578	62.4966	82.4225
V	44.5345	60.0887	60.4670	63.2251	71.5020	89.2511
VI	52.759	60.4674	60.8328	63.542	71.7525	89.4413

6. Conclusion

In the present work, first order shear deformation plate theory is developed for the accurate prediction of free vibration response of porous functionally graded plate. The material properties of porous FGM plate are obtained via modified power law. The governing differential equation using energy principle is obtained. The governing differential equation is discretized using DQM successfully. DQM has been used to examine the results for simply supported and clamped boundary conditions. The more specific conclusions as a result of the present studies are stated below:

- The convergence study indicates a reasonably less number of nodes required to get the desired accuracy.
- By increasing the porosity index, the fundamental frequency starts increasing for PD-2 and PD-5 and decreasing for PD-1, PD-3 and PD-4. The porosity index influence trend on the fundamental frequency is most pronounced in PD-4 and the least in PD-1.
- By increasing the grading index, the fundamental frequency of vibration of porous FGM circular plate decreases.
- With an increase in R_o/h ratio, fundamental frequency of vibration of porous FGM circular plate increases and the effect of R_o/h ratio is negligible after $R_o/h=50$.
- By increasing R_i/R_o ratio, the fundamental frequency of vibration of porous FGM circular plate increases.
- The fundamental frequency of vibration of porous FGM circular plate for clamped boundary condition is greater than the simply supported boundary condition but follows the same trend.

7. References

- [1] C. Steele, "Introduction to the Theory of Plates," p. 41.
- [2] M. Rakočević, "Bending of Laminated Composite Plates in Layerwise Theory," *Lamination - Theory and Application*, Dec. 2017, doi: 10.5772/intechopen.69975.
- [3] M.-O. Belarbi *et al.*, "On the Free Vibration Analysis of Laminated Composite and Sandwich Plates: A Layerwise Finite Element Formulation," *Latin American Journal of Solids and Structures*, vol. 14, no. 12, pp. 2265–2290, Dec. 2017, doi: 10.1590/1679-78253222.
- [4] Z. Cao, X. Liang, Y. Deng, X. Zha, R. Zhu, and J. Leng, "Novel Semi-Analytical Solutions for the Transient Behaviors of Functionally Graded Material Plates in the Thermal Environment," *Materials*, vol. 12, no. 24, Art. no. 24, Jan. 2019, doi: 10.3390/ma12244084.
- [5] M. Koizumi, "FGM activities in Japan," *Composites Part B: Engineering*, vol. 28, no. 1, pp. 1–4, Jan. 1997, doi: 10.1016/S1359-8368(96)00016-9.
- [6] I. M. El-Galy, B. I. Saleh, and M. H. Ahmed, "Functionally graded materials classifications and development trends from industrial point of view," *SN Appl. Sci.*, vol. 1, no. 11, p. 1378, Nov. 2019, doi: 10.1007/s42452-019-1413-4.
- [7] "THEORY OF PLATES AND SHELLS."
https://scholar.googleusercontent.com/scholar?q=cache:o1Ks4hWRQvMJ:scholar.google.com/+Timoshenko,+S.+and+Woinowsky-Krieger,+S.+%22Theory+of+plates+and+shells%22.+McGraw%E2%80%93Hill+New+York,+1959.&hl=en&as_sdt=0,5
- [8] A. E. H. Love and G. H. Darwin, "XVI. The small free vibrations and deformation of a thin elastic shell," *Philosophical Transactions of the Royal Society of London. (A.)*, vol. 179, pp. 491–546, Jan. 1888, doi: 10.1098/rsta.1888.0016.
- [9] G. Kirchhoff, "Über das Gleichgewicht und die Bewegung einer elastischen Scheibe.," *Journal für die reine und angewandte Mathematik (Crelles Journal)*, vol. 1850, no. 40, pp. 51–88, Jul. 1850, doi: 10.1515/crll.1850.40.51.
- [10] E. REISSNER, "The effect of transverse shear deformation on the bending of elastic plates," *J. Appl. Mech.*, pp. A69–A77, 1945.
- [11] R. D. MINDLIN, "Influence of Rotatory Inertia and Shear on Flexural Motions of Isotropic, Elastic Plates," *J. Appl. Mech.*, vol. 18, pp. 31–38, 1951.
- [12] J. M. Whitney, "Stress Analysis of Thick Laminated Composite and Sandwich Plates," *Journal of Composite Materials*, vol. 6, no. 3, pp. 426–440, Jul. 1972, doi: 10.1177/002199837200600301.
- [13] R. Bellman and J. Casti, "Differential quadrature and long-term integration," *Journal of Mathematical Analysis and Applications*, vol. 34, no. 2, pp. 235–238, May 1971, doi: 10.1016/0022-247X(71)90110-7.
- [14] F. Civan, "Solving multivariable mathematical models by the quadrature and cubature methods," *Numerical Methods for Partial Differential Equations*, vol. 10, no. 5, pp. 545–567, 1994, doi: 10.1002/num.1690100503.
- [15] C. W. Bert, W. Xinwei, and A. G. Striz, "Differential quadrature for static and free vibration analyses of anisotropic plates," *International Journal of Solids and Structures*, vol. 30, no. 13, pp. 1737–1744, Jan. 1993, doi: 10.1016/0020-7683(93)90230-5.
- [16] S. K. Jang, C. W. Bert, and A. G. Striz, "Application of differential quadrature to static analysis of structural components," *International Journal for Numerical Methods in Engineering*, vol. 28, no. 3, pp. 561–577, 1989, doi: 10.1002/nme.1620280306.

- [17] H. Du, M. K. Lim, and R. M. Lin, "Application of generalized differential quadrature method to structural problems," *International Journal for Numerical Methods in Engineering*, vol. 37, no. 11, pp. 1881–1896, 1994, doi: 10.1002/nme.1620371107.
- [18] F. Civan and C. M. Sliepcevich, "Application of differential quadrature to transport processes," *Journal of Mathematical Analysis and Applications*, vol. 93, no. 1, pp. 206–221, Apr. 1983, doi: 10.1016/0022-247X(83)90226-3.
- [19] T. C. Fung, "Solving initial value problems by differential quadrature method—part 1: first-order equations," *International Journal for Numerical Methods in Engineering*, vol. 50, no. 6, pp. 1411–1427, 2001, doi: 10.1002/1097-0207(20010228)50:6<1411::AID-NME78>3.0.CO;2-O.
- [20] T. C. Fung, "Solving initial value problems by differential quadrature method—part 2: second- and higher-order equations," *International Journal for Numerical Methods in Engineering*, vol. 50, no. 6, pp. 1429–1454, 2001, doi: 10.1002/1097-0207(20010228)50:6<1429::AID-NME79>3.0.CO;2-A.
- [21] T. C. Fung, "Stability and accuracy of differential quadrature method in solving dynamic problems," *Computer Methods in Applied Mechanics and Engineering*, vol. 191, no. 13, pp. 1311–1331, Jan. 2002, doi: 10.1016/S0045-7825(01)00324-3.
- [22] M. Golchi, M. Talebitooti, and R. Talebitooti, "Thermal buckling and free vibration of FG truncated conical shells with stringer and ring stiffeners using differential quadrature method," *Mechanics Based Design of Structures and Machines*, vol. 47, no. 3, pp. 255–282, May 2019, doi: 10.1080/15397734.2018.1545588.
- [23] P. Malekzadeh and M. Ghaedsharaf, "Three-dimensional free vibration of laminated cylindrical panels with functionally graded layers," *Composite Structures*, vol. 108, pp. 894–904, Feb. 2014, doi: 10.1016/j.compstruct.2013.10.024.
- [24] P. Zahedinejad, P. Malekzadeh, M. Farid, and G. Karami, "A semi-analytical three-dimensional free vibration analysis of functionally graded curved panels," *International Journal of Pressure Vessels and Piping*, vol. 87, no. 8, pp. 470–480, Aug. 2010, doi: 10.1016/j.ijpvp.2010.06.001.
- [25] M. Farid, P. Zahedinejad, and P. Malekzadeh, "Three-dimensional temperature dependent free vibration analysis of functionally graded material curved panels resting on two-parameter elastic foundation using a hybrid semi-analytic, differential quadrature method," *Materials & Design*, vol. 31, no. 1, pp. 2–13, Jan. 2010, doi: 10.1016/j.matdes.2009.07.025.
- [26] G. Venkateswara Rao, K. Kanaka Raju, and I. S. Raju, "Finite element formulation for the large amplitude free vibrations of beams and orthotropic circular plates," *Computers & Structures*, vol. 6, no. 3, pp. 169–172, Jun. 1976, doi: 10.1016/0045-7949(76)90025-0.
- [27] K. K. Raju and G. V. Rao, "Axisymmetric vibrations of circular plates including the effects of geometric non-linearity, shear deformation and rotary inertia," *Journal of Sound and Vibration*, vol. 47, no. 2, pp. 179–184, Jul. 1976, doi: 10.1016/0022-460X(76)90716-1.
- [28] G. V. Rao and K. K. Raju, "Large amplitude axisymmetric vibrations of orthotropic circular plates elastically restrained against rotation," *Journal of Sound and Vibration*, vol. 69, no. 2, pp. 175–180, Mar. 1980, doi: 10.1016/0022-460X(80)90604-5.
- [29] X. WANG, J. YANG, and J. XIAO, "On free vibration analysis of circular annular plates with non-uniform thickness by the differential quadrature method," *J. sound vib*, vol. 184, no. 3, pp. 547–551, 1995.
- [30] E. Romanelli, R. E. Rossi, P. A. A. Laura, and R. H. Gutierrez, "TRANSVERSE VIBRATIONS OF A CIRCULAR ANNULAR PLATE WITH AN INTERMEDIATE

- CIRCULAR SUPPORT AND A FREE INNER EDGE,” *Journal of Sound and Vibration*, vol. 212, no. 3, pp. 564–571, May 1998, doi: 10.1006/jsvi.1997.1452.
- [31] H. Z. GU and X. W. WANG, “On the free vibration analysis of circular plates with stepped thickness over a concentric region by the differential quadrature element method,” *J. sound vib*, vol. 202, no. 3, pp. 452–459, 1997.
- [32] K. M. Liew, J.-B. Han, and Z. M. Xiao, “VIBRATION ANALYSIS OF CIRCULAR MINDLIN PLATES USING THE DIFFERENTIAL QUADRATURE METHOD,” *Journal of Sound and Vibration*, vol. 205, no. 5, pp. 617–630, Sep. 1997, doi: 10.1006/jsvi.1997.1035.
- [33] T. Y. Wu and G. R. Liu, “Free vibration analysis of circular plates with variable thickness by the generalized differential quadrature rule,” *International Journal of Solids and Structures*, vol. 38, no. 44, pp. 7967–7980, Nov. 2001, doi: 10.1016/S0020-7683(01)00077-4.
- [34] J. Wang, K. M. Liew, M. J. Tan, and S. Rajendran, “Analysis of rectangular laminated composite plates via FSDT meshless method,” *International Journal of Mechanical Sciences*, vol. 44, no. 7, pp. 1275–1293, Jul. 2002, doi: 10.1016/S0020-7403(02)00057-7.
- [35] M. M. Najafizadeh and M. R. Eslami, “Buckling analysis of circular plates of functionally graded materials under uniform radial compression,” *International Journal of Mechanical Sciences*, vol. 44, no. 12, pp. 2479–2493, Dec. 2002, doi: 10.1016/S0020-7403(02)00186-8.
- [36] T. Y. Wu, Y. Y. Wang, and G. R. Liu, “Free vibration analysis of circular plates using generalized differential quadrature rule,” *Computer Methods in Applied Mechanics and Engineering*, vol. 191, no. 46, pp. 5365–5380, Nov. 2002, doi: 10.1016/S0045-7825(02)00463-2.
- [37] K. M. Liew, Y. Q. Huang, and J. N. Reddy, “Vibration analysis of symmetrically laminated plates based on FSDT using the moving least squares differential quadrature method,” *Computer Methods in Applied Mechanics and Engineering*, vol. 192, no. 19, pp. 2203–2222, May 2003, doi: 10.1016/S0045-7825(03)00238-X.
- [38] M. Haterbouch and R. Benamar, “Geometrically nonlinear free vibrations of simply supported isotropic thin circular plates,” *Journal of Sound and Vibration*, vol. 280, no. 3, pp. 903–924, Feb. 2005, doi: 10.1016/j.jsv.2003.12.051.
- [39] S. S. Vel and R. C. Batra, “Three-dimensional exact solution for the vibration of functionally graded rectangular plates,” *Journal of Sound and Vibration*, vol. 272, no. 3, pp. 703–730, May 2004, doi: 10.1016/S0022-460X(03)00412-7.
- [40] R. C. BATRA and J. JIN, “Natural frequencies of a functionally graded anisotropic rectangular plate,” *J. sound vib*, vol. 282, no. 1–2, pp. 509–516, 2005.
- [41] A. M. Zenkour, “Generalized shear deformation theory for bending analysis of functionally graded plates,” *Applied Mathematical Modelling*, vol. 30, no. 1, pp. 67–84, Jan. 2006, doi: 10.1016/j.apm.2005.03.009.
- [42] U. S. Gupta, R. Lal, and S. Sharma, “Vibration analysis of non-homogeneous circular plate of nonlinear thickness variation by differential quadrature method,” *Journal of Sound and Vibration*, vol. 298, no. 4, pp. 892–906, Dec. 2006, doi: 10.1016/j.jsv.2006.05.030.
- [43] F. Ebrahimi and A. Rastgo, “An analytical study on the free vibration of smart circular thin FGM plate based on classical plate theory,” *Thin-Walled Structures*, vol. 46, no. 12, pp. 1402–1408, Dec. 2008, doi: 10.1016/j.tws.2008.03.008.
- [44] H. S. Yalcin, A. Arikoglu, and I. Ozkol, “Free vibration analysis of circular plates by differential transformation method,” *Applied Mathematics and Computation*, vol. 212, no. 2, pp. 377–386, Jun. 2009, doi: 10.1016/j.amc.2009.02.032.

- [45] E. Carrera, S. Brischetto, M. Cinefra, and M. Soave, "Refined and Advanced Models for Multilayered Plates and Shells Embedding Functionally Graded Material Layers," *Mechanics of Advanced Materials and Structures*, vol. 17, no. 8, pp. 603–621, Nov. 2010, doi: 10.1080/15376494.2010.517730.
- [46] M. K. Singha, T. Prakash, and M. Ganapathi, "Finite element analysis of functionally graded plates under transverse load," *Finite Elements in Analysis and Design*, vol. 47, no. 4, pp. 453–460, Apr. 2011, doi: 10.1016/j.finel.2010.12.001.
- [47] Y. Kiani, A. H. Akbarzadeh, Z. T. Chen, and M. R. Eslami, "Static and dynamic analysis of an FGM doubly curved panel resting on the Pasternak-type elastic foundation," *Composite Structures*, vol. 94, no. 8, pp. 2474–2484, Jul. 2012, doi: 10.1016/j.compstruct.2012.02.028.
- [48] G. Castellazzi, C. Gentilini, P. Krysl, and I. Elishakoff, "Static analysis of functionally graded plates using a nodal integrated finite element approach," *Composite Structures*, vol. 103, pp. 197–200, Sep. 2013, doi: 10.1016/j.compstruct.2013.04.013.
- [49] H.-T. Thai and D.-H. Choi, "Analytical solutions of refined plate theory for bending, buckling and vibration analyses of thick plates," *Applied Mathematical Modelling*, vol. 37, no. 18, pp. 8310–8323, Oct. 2013, doi: 10.1016/j.apm.2013.03.038.
- [50] G. Duan, X. Wang, and C. Jin, "Free vibration analysis of circular thin plates with stepped thickness by the DSC element method," *Thin-Walled Structures*, vol. 85, pp. 25–33, Dec. 2014, doi: 10.1016/j.tws.2014.07.010.
- [51] B. V. Farahani, J. M. Berardo, R. Drgas, J. M. A. C. de Sá, A. J. M. Ferreira, and J. Belinha, "The Axisymmetric Analysis of Circular Plates Using the Radial Point Interpolation Method," *International Journal for Computational Methods in Engineering Science and Mechanics*, vol. 16, no. 6, pp. 336–353, Nov. 2015, doi: 10.1080/15502287.2015.1103819.
- [52] Q. Wang, D. Shi, Q. Liang, and X. Shi, "A unified solution for vibration analysis of functionally graded circular, annular and sector plates with general boundary conditions," *Composites Part B: Engineering*, vol. 88, pp. 264–294, Mar. 2016, doi: 10.1016/j.compositesb.2015.10.043.
- [53] K. K. Żur, "Quasi-Green's function approach to free vibration analysis of elastically supported functionally graded circular plates," *Composite Structures*, vol. 183, pp. 600–610, Jan. 2018, doi: 10.1016/j.compstruct.2017.07.012.
- [54] S. Khare and N. D. Mittal, "Axisymmetric bending and free vibration of symmetrically laminated circular and annular plates having elastic edge constraints," *Ain Shams Engineering Journal*, vol. 10, no. 2, pp. 343–352, Jun. 2019, doi: 10.1016/j.asej.2018.10.006.
- [55] M. Z. Roshanbakhsh, S. M. Tavakkoli, and B. Navayi Neya, "Free vibration of functionally graded thick circular plates: An exact and three-dimensional solution," *International Journal of Mechanical Sciences*, vol. 188, p. 105967, Dec. 2020, doi: 10.1016/j.ijmecsci.2020.105967.
- [56] N. Wattanasakulpong, B. Gangadhara Prusty, D. W. Kelly, and M. Hoffman, "Free vibration analysis of layered functionally graded beams with experimental validation," *Materials & Design (1980-2015)*, vol. 36, pp. 182–190, Apr. 2012, doi: 10.1016/j.matdes.2011.10.049.
- [57] Y. Q. Wang, Y. H. Wan, and Y. F. Zhang, "Vibrations of longitudinally traveling functionally graded material plates with porosities," *European Journal of Mechanics - A/Solids*, vol. 66, pp. 55–68, Nov. 2017, doi: 10.1016/j.euromechsol.2017.06.006.
- [58] M. C. Kiran, S. C. Kattimani, and M. Vinyas, "Porosity influence on structural behaviour of skew functionally graded magneto-electro-elastic plate," *Composite Structures*, vol. 191, pp. 36–77, May 2018, doi: 10.1016/j.compstruct.2018.02.023.

- [59] F. Ebrahimi, A. Jafari, and M. R. Barati, "Vibration analysis of magneto-electro-elastic heterogeneous porous material plates resting on elastic foundations," *Thin-Walled Structures*, vol. 119, pp. 33–46, Oct. 2017, doi: 10.1016/j.tws.2017.04.002.
- [60] M. R. Barati, H. Shahverdi, and A. M. Zenkour, "Electro-mechanical vibration of smart piezoelectric FG plates with porosities according to a refined four-variable theory," *Mechanics of Advanced Materials and Structures*, vol. 24, no. 12, pp. 987–998, Sep. 2017, doi: 10.1080/15376494.2016.1196799.
- [61] M. C. Kiran and S. C. Kattimani, "Assessment of porosity influence on vibration and static behaviour of functionally graded magneto-electro-elastic plate: A finite element study," *European Journal of Mechanics - A/Solids*, vol. 71, pp. 258–277, Sep. 2018, doi: 10.1016/j.euromechsol.2018.04.006.
- [62] J. Zhao, K. Choe, F. Xie, A. Wang, C. Shuai, and Q. Wang, "Three-dimensional exact solution for vibration analysis of thick functionally graded porous (FGP) rectangular plates with arbitrary boundary conditions," *Composites Part B: Engineering*, vol. 155, pp. 369–381, Dec. 2018, doi: 10.1016/j.compositesb.2018.09.001.
- [63] K. M. Liew, J.-B. Han, and Z. M. Xiao, "Differential quadrature method for thick symmetric cross-ply laminates with first-order shear flexibility," *International Journal of Solids and Structures*, vol. 33, no. 18, pp. 2647–2658, Jul. 1996, doi: 10.1016/0020-7683(95)00174-3.
- [64] M. Mohammadi, M. Ghayour, and A. Farajpour, "Free transverse vibration analysis of circular and annular graphene sheets with various boundary conditions using the nonlocal continuum plate model," *Composites Part B: Engineering*, vol. 45, no. 1, pp. 32–42, Feb. 2013, doi: 10.1016/j.compositesb.2012.09.011.
- [65] N.-T. Nguyen, D. Hui, J. Lee, and H. Nguyen-Xuan, "An efficient computational approach for size-dependent analysis of functionally graded nanoplates," *Computer Methods in Applied Mechanics and Engineering*, vol. 297, pp. 191–218, Dec. 2015, doi: 10.1016/j.cma.2015.07.021.
- [66] C. H. Thai, A. J. M. Ferreira, and P. Phung-Van, "A nonlocal strain gradient isogeometric model for free vibration and bending analyses of functionally graded plates," *Composite Structures*, vol. 251, p. 112634, Nov. 2020, doi: 10.1016/j.compstruct.2020.112634.
- [67] C. Y. Dong, "Three-dimensional free vibration analysis of functionally graded annular plates using the Chebyshev–Ritz method," *Materials & Design*, vol. 29, no. 8, pp. 1518–1525, Jan. 2008, doi: 10.1016/j.matdes.2008.03.001.